Molecular Genetics and Metabolism 95 (2008) 182–187

Contents lists available at ScienceDirect

Molecular Genetics and Metabolism

journal homepage: www.elsevier.com/locate/ymgme

Case report of familial Carney complex due to novel frameshift mutation c.597del C (p.Phe200LeufsX6) in *PRKAR1A*

Akihiko Sasaki [a], Yukio Horikawa [a,b,*], Tetsuya Suwa [a], Mayumi Enya [a], Shin-ichi Kawachi [a], Jun Takeda [a]

[a] Department of Diabetes and Endocrinology, Division of Molecule and Structure, Gifu University School of Medicine, 1-1 Yanagido, Gifu 501-1194, Japan
[b] Laboratory of Medical Genomics, Biosignal Genome Resource Center, Institute for Molecular and Cellular Regulation, Gunma University, Maebashi, Japan

ARTICLE INFO

Article history:
Received 4 June 2008
and in revised form 22 July 2008
Accepted 22 July 2008
Available online 29 August 2008

Keywords:
Carney complex
PRKAR1A
Mutation
Cushing syndrome
Acromegaly
PPNAD

ABSTRACT

Carney complex is an autosomal dominantly inherited disease characterized by skin pigmentation, myxoma, primary pigmented nodular adrenocortical disease (PPNAD), and acromegaly. However, only a few incidences of PPNAD combined with acromegaly are observed in patients. The type 1α regulatory subunit of cAMP-dependent protein kinase (*PRKAR1A*) has been identified in patients as a causative gene for Carney complex by a positional cloning approach. Here, we report a female patient diagnosed with Cushing's syndrome and a GH-producing pituitary adenoma without otherwise evident acromegaly that could be diagnosed only by specialized endocrinological tests. Based on family history of acromegaly (mother and sister) and the fact that the combination of both diseases is very rare, genetic diagnosis involving Carney complex was considered to be appropriate. The 10 exons and flanking regions of *PRKAR1A* were screened for mutations by direct DNA sequencing. The patient and her mother and sister were found to have the same, novel frameshift mutation resulting from a single base deletion in exon 6 coding cAMP-binding domain A, denoted c.597delC in *PRKAR1A*. This single base deletion generated an immature stop codon at the sixth codon (p.Phe200LeufsX6). Even family members with the same mutation can show distinct phenotypes, suggesting that Carney complex is a multifactorial disorder comprising various genetic and environmental factors. Genetic diagnosis makes it possible to prepare more effective therapeutic strategies for patients and gene carriers and to avoid unnecessary tests for non-carriers in the family of the patient.

Introduction

Carney et al. of the Mayo Clinic identified adrenocortical hyperplasia with pigmentation in bilateral adrenal glands, namely, primary pigmented nodular adrenocortical disease (PPNAD), in patients with Cushing's syndrome in 1984. In the following year, they reported four patients presenting with the same findings regarding pigmentation, cardiac myxoma, and familial incidence pattern, and reported these symptoms as a syndrome [1]. Kirschner et al. identified *PRKAR1A* as a causative gene for this syndrome, which is currently given the generic name Carney complex in 2000 [2]. *PRKAR1A* protein is a regulatory subunit of a holoenzyme, cAMP-dependent protein kinase A. Mutations in *PRKAR1A* are found in approximately 70% of patients with Carney complex; however, Carney complex is a syndrome that may well involve other unknown genes. Stratakis et al. reported the major clinical findings and their frequencies of occurrence in a study involving 338 patients with Carney complex. Pigmentation was found in approximately 80% of the patients, while the incidence of cardiac myxoma, PPNAD, and acromegaly, which are considered characteristic findings of the syndrome, was not as high [3]. However, it is possible that the study included patients who had not yet shown symptoms or who had imprecise assessment of endocrine parameters.

While PPNAD is very rarely seen in Cushing's syndrome, it is the most frequently observed endocrine disorder in patients with Carney complex. Histopathological findings literally show blackish-brown nodules of various sizes at multiple sites in the adrenal glands. Diagnosis of the disease by imaging modalities, such as CT scan, is difficult because the size and weight of the diseased adrenal glands are almost the same as those of normal adrenal glands. As an endocrinological characteristic, PPNAD, unlike typical adrenal Cushing's syndrome, is known to show a paradoxical increase in glucocorticoid secretion by dexamethazone suppression test. This increase was also evident in our patient described below. However, since there are reports of patients who showed no glucocorticoid hyperproduction yet were found to have PPNAD at autopsy, the only way to obtain a reliable diagnosis of the disease is by biopsy.

Acromegaly associated with growth hormone-producing pituitary adenoma is the second most frequently-observed endocrine disorder in patients with Carney complex. On the other hand, there

* Corresponding author. Fax: +81 58 230 6376.
E-mail address: yhorikaw@gifu-u.ac.jp (Y. Horikawa).

1096-7192/$ - see front matter © 2008 Elsevier Inc. All rights reserved.
doi:10.1016/j.ymgme.2008.07.009

also have been reports of patients who do not have acromegaly yet show hyperproduction of growth hormone, as well as of patients who develop prolactin-producing pituitary adenomas. Other reported complications associated with Carney complex include various types of tumors, such as Sertoli cell tumor in male patients, thyroid tumor (non-medullary carcinoma), schwannoma, and ductal adenoma of the breast [3].

Although an analysis of family members performed in 1996 revealed that Carney syndrome is an autosomal, dominantly inherited disease and the chromosome 2p gene locus was identified by linkage analysis [4], the association of this gene with the syndrome is not yet established. Subsequently, the chromosome 17q24 gene locus was identified in 1998 [5], and *PRKAR1A* was later identified as a causative gene by a positional cloning approach in 2000 [2]. Recently, mutations in a phosphodiesterase gene also were associated with adrenocortical changes similar to those in PPNAD in patients with genetic forms of adrenocortical Cushing syndrome [6].

PRKAR1A protein is one of the regulatory subunits of protein kinase A (PKA), a cAMP-dependent kinase. PKA is a holoenzyme comprising a tetramer of two units having three isoforms (Cα, Cβ and Cγ) that are responsible for its catalytic activity, and two regulatory subunits that have four isoforms (RIα, RIβ, RIIα and RIIβ). Depending on the combination of these subunits, PKA is classified into Type I (the regulatory subunit consisting of a dimer of RIα or RIβ) and Type II (the regulatory subunit consisting of a dimer of RIIα or RIIβ) [7]. Both types of PKA are co-expressed in almost all tissues, but their expression levels differ among tissues. The α-subunit is expressed in almost all tissues, while the β-subunit is expressed at a high level in particular tissues, such as brain and fat tissue. PKA is inactive in the tetrameric state, and exerts its enzymatic activity when cAMP binds to the regulatory subunit and subsequently separates it from the catalytic subunit [8]. The regulatory subunit RIα protein coded by *PRKAR1A* is composed of four domains. Although various gene defects have been reported in relation to this syndrome, no relationship between these mutations and the phenotypes has been demonstrated [9]. The mutations are found over the entire region of the gene, but are somewhat concentrated in cAMP-binding domain A.

Methods

Mutation analysis

The ten exons and flanking regions of *PRKAR1A* were screened for mutations by direct DNA sequencing of the amplified polymerase chain reaction (PCR) products, using specific primer pairs and an ABI PRISM BigDye Terminator Cycle Sequencing FS ready Reaction Kit (Applied Biosystems, Foster City, CA). Primer pairs and PCR conditions used for screening of *PRKAR1A* are available in Table 1. Genomic DNA extracted from subjects was initially denatured at 95 °C for 1 min, followed by 35 cycles of denaturation at 94 °C for 30 s, annealing at 58–67 °C for 30 s, extension at 72 °C for 30 s, and a final extension step of 7 min. The sequencing reactions were analyzed by automatic DNA sequencers (Applied Biosystems model 3100). Informed consent was obtained from all family members.

Endocrinological tests

The responses of plasma pituitary hormone levels to the administration of respective hypothalamic stimulating hormones were examined. After drawing basal plasma samples through a plastic canula inserted into the antecubital vein following a one hour bed rest, 500 μg TRH[1] (TRH injection, Mitsubishi Tanabe Pharma Corporation, Osaka, Japan), 100 μg hCRH (hCRH injection, Mitsubishi Tanabe Pharma Corporation) or 100 μg hGRH (GRF injection, Dainippon Sumitomo Pharma Co., Ltd, Osaka, Japan) was iv administered. Plasma samples were obtained after 15, 30, 60, 90 and 120 min.

[1] *Abbreviations used:* TRH, thyrotropin-releasing hormone; GRH, growth hormone-releasing hormone; CRH, corticotropin-releasing hormone.

Table 1
PCR primers used for mutation screening of the human *PRKAR1A* gene

Primer	Product size	Annealing
ex1-F: TTGACTTTTGTGCCCTGGTA	1330	58
ex1-R: CTTTTTCATTCATCGTTTCT		
ex2-F: TCTTGGATCACTATGTTGG	1030	58
ex2-R: CAGGACAAATGAGGCTCGTA		
ex3/4-F: TTCTCCTCCTCCAC CAACC	1300	67
ex3/4-R: TCGCCTCCTCTCCCGTAACA		
ex5-F: TACGGGAGAGGAGGCGAGAC	1500	62
ex5-R: ACACAACAGAGAAGAATAGG		
ex6-F: TTACATCCTTACAGAGTGCT	650	61
ex6-R: CCAAACATGAGATGACCAG		
ex7-F: TCAAAGAAGGAAGAGGTAG	900	61
ex7-R: CAGGGGGAATGAGTAGCAA		
ex8-F: ATGCTTTGTGTTTTGGATA	1100	62
ex8-R: GTTGAGACTTTGCGAATGA		
ex9-F: AGGGAGAACCAGGGGATGA	1400	62
ex9-R: TGTTTCGTTTGAGGATGTC		
ex10-F: TGAAATTGCACTACTGATGA	750	58
ex10-R: TGGCAAACAACAACTCTGG		

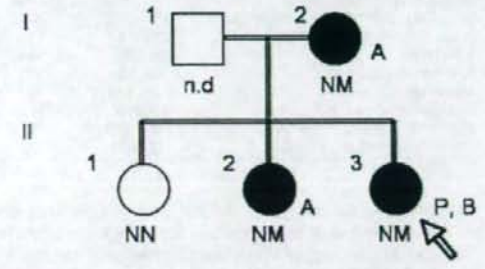

P: PPNAD
A: Acromegaly
B: Biochemical acromegaly (GH-producing pituitary adenoma without evident acromegaly)
N: Normal allele
M: p.Phe200LeufsX6 mutation
n.d.: not done

Fig. 1. Pedigree of this Carney complex case. The subjects, I-2, II-1, II-2 and II-3 underwent *PRKAR1A* analysis. Informed consent was not obtained from I-1 subject.

Case report

Proband (II-3)

The patient is 27-year-old female, and presented with amenorrhea at 23 years of age. She has a history of urinary tract stones. She has a family history of acromegaly in her mother and sister (Fig. 1). The patient is the third of three sisters. The patient's history includes diagnosis with bilateral glaucoma at 18 years and hypertension at 20 years, but she did not receive any treatment. Since then, she has become aware of such symptoms as irregular menstruation, hirsutism, buffalo hump, moon face, and red lines on the skin in the abdominal region. These changes had also been pointed out to her by people around her. Her mother and sister were diagnosed with acromegaly, which brought her to our department for examination. At that time we did not note any findings suggestive of acromegaly, and therefore decided to observe her clinical course. She was later found to have osteoporosis at a nearby hospital. She then returned to our department complaining of lack of

Table 2
Examination findings at the time of admission

Variable	Normal range	Values in patient
Sodium (mmol/l)	135–147	143
Potassium (mmol/l)	3.5–4.8	3.7
Chloride (mmol/l)	97–108	105
Urea nitrogen (mmol/l)	2.9–7.1	4.1
Creatinine (μmol/l)	35.4–70.7	60.1
Fasting plasma glucose (mmol/l)	3.9–6.1	5.4
HbA1c (%)	4.3–5.8	5.8
Calcium (mmol/l)	2.0–2.5	2.3
Protein (g/l)	65–82	63
Albumin (g/l)	39–49	43
Alkaline phosphatase (IU/l)	130–330	414
Aspartate aminotransferase (IU/l)	7–35	29
Alanine aminotransferase (IU/l)	7–40	71
Lactate dehydrogenase (IU/l)	125–225	375
Total bilirubin (μmol/l)	3.4–20.5	15.4
LDL-cholesterol (mmol/l)	1.8–3.6	3.7
HDL-chokesterol (mmol/l)	1.0–1.9	1.8
Triglyceride (mmol/l)	0.57–1.7	0.95
Plasma corticotropin (pmol/l)	1.6–12.3	<1.1
Plasma aldosterone (pmol/l)	82.9–441	332.9
Plasma renin activity (ng/l/s)	0.083–0.805	1.36
Dehydroepiandrosterone sulfate (μmol/l)	23.1–81.1	20.2
Plasma growth hormone (μg/l)	0.28–1.64	1.19
IGF-I (ng/ml)	119–389	380
IGFBP-3 (μg/ml)	1.99–3.20	2.03
Thyrotropin (μU/ml)	0.35–4.94	0.28
Free thyroxine (pmol/l)	9.0–19.0	11.2
Plasma prolactine (pmol/l)	266.1–1327.8	395.6
24 h urinary cortisol (μg/24h)	11.2–80.3	373

Table 3
Various load tests of the proband at this admission

Clock time	Diurnal rhythm			Dexamethasone 8 mg suppression test
	8:00	14:00	23:00	8:00
ACTH (pmol/l)	<1.1	<1.1	<1.1	<1.1
Cortisol (nmol/l)	562.8	631.8	656.6	902.2
	0 min	30 min	60 min	120 min
75 g oral glucose tolerance test (in 2002)				
PG (mmol/l)	5.7	8.4	10.5	6.7
IRI (pmol/l)	67.4	680.6	833.4	638.9
GH (μg/l)	1.05	0.88	0.92	1.42
75 g oral glucose tolerance test				
PG (mmol/l)	4.3	11.4	14.5	11.9
IRI (pmol/l)	120.8	986.2	1298.7	1282.1
GH (μg/l)	5.92	1.70	1.12	2.61

	0 min	15 min	30 min	60 min	90 min	120 min
TRH test						
TSH (mU/l)	0.38	2.81	3.83	3.27	2.23	1.56
PRL (μg/l)	13.7	78.9	55.9	29.8	18.5	12.6
GH (μg/l)	1.45	4.59	3.97	3.05	3.15	1.62
GRH test						
GH (μg/l)	3.40	9.79	6.52	5.42	4.38	4.21
CRH test						
ACTH (pmol/l)	<1.1	<1.1	<1.1	<1.1	<1.1	<1.1
Cortisol (nmol/l)	648.4	700.8	703.5	662.2	623.5	667.7

menstruation for two years. At that time she showed low serum ACTH level and high serum cortisol level, and was admitted to our hospital. At the time of admission she had mild obesity, hypertension, and Cushing's syndrome. She also showed a small pigmented spot in the lips. The general examination findings at the time of admission are shown in Table 2. The patient showed decreased bone density, but ultrasound of the thyroid gland revealed no abnormal findings.

Regarding the results of blood biochemistry at the time of admission, the patient showed a high level of LDL cholesterol. The serum potassium level hovered between 3 and 4 mEq/L during the period of hospitalization. The patient's ACTH level was lower than the limit of measurement sensitivity. Blood and urine cortisol and urine 17-OHCS levels were high. The IGF-1 level was near the higher limit of the normal range, while the TSH level was low. We then examined the circadian changes of the endocrine parameters and also performed a dexamethazone suppression test. The patient did not exhibit circadian changes in either the ACTH or cortisol levels, but showed an increase in cortisol level to 902.2 nmol/l on the morning following administration of 8 mg of dexamethazone. The results of various load tests are shown in Table 3. In the OGTT test performed in 2002, the patient showed normal glucose tolerance, although the glucose level at 1 h was high at 10.5 mmol/l. The GH level also was suppressed to less than 1 ng/mL. However, in the glucose tolerance test performed during the hospitalization period, the patient showed a diabetic pattern and marked hyperinsulinemia. Regarding the GH level, it was suppressed but not less than 1 μg/l; in TRH stimulation test, the patient showed an increased level that was determined to be a paradoxical response (positive in approximately 80% of patients). No changes in the GH level were observed in bromocriptine test (decreased in approximately 80% of patients, increased in normal people). In GRH stimulation test, the GH level was increased 2.5-fold to the reference value, which is a normal response. In CRH stimulation test, no change in the ACTH level was observed.

Adosterol scintigraphy showed uptake into the bilateral adrenal glands with no difference between the left and the right (Fig. 2A). The results of imaging examinations of the adrenal glands are shown in Fig. 2B. Both the MRI and CT images can give the impression that both adrenal glands are somewhat large, but they were within normal range according to physical measurement. MRI of the pituitary gland revealed a low intensity area of 9 mm in the right side during an early phase of contrast enhancement (Fig. 2C).

Based on these results, the patient was diagnosed with Cushing's syndrome due to cortisol production from the bilateral adrenal glands and a GH-producing pituitary adenoma without evident acromegaly. Based on the family history of acromegaly (mother and sister) and the fact that the combination of both of the diseases are rare, a diagnosis involving Carney complex was investigated by direct DNA sequencing of *PRKAR1A*. Carney complex is an autosomal dominantly inherited disease characterized by skin pigmentation, myxoma, PPNAD, and acromegaly. The first-line treatment for PPNAD is bilateral adrenalectomy. Therefore, to make a definite diagnosis, we carried out a gene analysis after giving explanations to the patient and her family and obtaining informed consent from the patient. A causative gene of Carney complex, called the protein kinase A regulatory subunit 1α gene or *PRKAR1A*, is a gene consisting of 10 exons located on the long arm of the seventeenth chromosome. The patient in this case also had a novel frameshift mutation resulting from a single base deletion in exon 6, denoted as c.597delC. We found that this single base deletion caused a frameshift, which generated a stop codon at the sixth codon (p.Phe200LeufsX6), as shown in Fig. 3. The same deletion was also found in her mother and the second sister. Based on these results, the patient was diagnosed with Carney complex, and the change in the adrenal glands was determined to be due to PPNAD. The patient subsequently underwent laparoscopic bilateral adrenalectomy at the urology department of our hospital. A specimen of excised adrenal gland obtained from this patients and histological image is shown in Fig. 4A and B. Macroscopic observation of both adrenal glands shows black-pigmented nodules of various sizes. The cross-section surface shows the same phenomenon. Histopathological findings include marked atrophy of the zona fasciculate and nodules of eosinophilic cells in the zona reticularis. Lipofuscin deposition and hyperplasia of fat cells were also observed. These findings confirmed the diagnosis of PPNAD. Since the surgery, the patient has been observed while

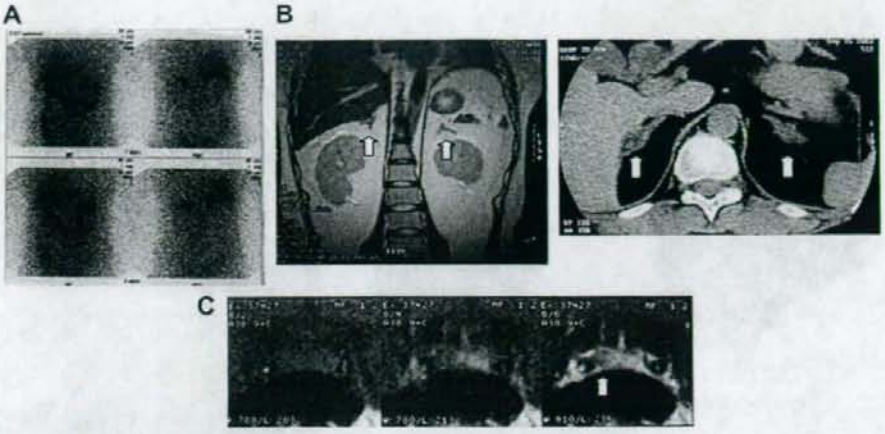

Fig. 2. Imaging findings in the proband. (A) Adosterol Scintigraphy: Evident uptake was found in bilateral adrenal glands. (B) Abdominal MRI and CT scan: No evident abnormality was found in bilateral adrenal glands. (C) Pituitary MRI: Low intensity nodule of 9 × 7 mm size was found in right side of pituitary.

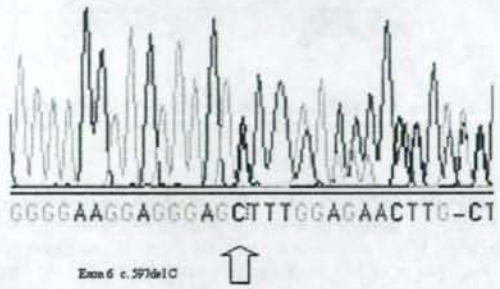

Fig. 3. Detection of a novel frameshift mutation, c.597delC in *PRKAR1A* exon 6.

receiving a steroid substitution therapy with hydrocortisone, and is showing significant improvement in the symptoms of Cushing's syndrome and hypertension exhibited at the time of admission. We are presently observing the clinical course of the GH-producing pituitary adenoma while considering the use of a somatostatin analogue.

Proband's mother (I-2)

She is 61 years old, and was diagnosed with acromegaly as well as parotid gland tumor at 40 years of age. She received the Hardy operation for somatotroph adenoma at 51 years of age, but the growth hormone level did not decrease to normal level although the IGF-1 level was near the higher limit of normal range. She came to our hospital not taking any medication and has not shown any abnormal findings in physical condition or laboratory data related to adrenal abnormality (Table 4A). Since she also has the mutation of *PRKAR1A*, we plan to follow her clinical course carefully in the future.

Proband's older sister (II-2)

Her older sister is 29 years old, and was diagnosed with acromegaly at 21 years of age when she presented with galactorrhea. She received the Hardy operation 4 years later. Her growth hormone level did not decrease to normal level. She also has the mutation of *PRKAR1A*, and sometimes shows a higher level of serum cortisol (Table 4B). She has not yet shown any abnormal findings in adrenals by abdominal CT scan. At 27 years of age, she started the somatostatin analogue, octreotide, Sandstatin LAR™ (Novartis, Switzerland) injection 20 μg/month, which is meant to decrease the cAMP level in cytosol by inhibiting adenylate cyclase, but her serum level of growth hormone and IGF-1 is still higher than the normal range. However, we found a necrotized image of her residual pituitary gland by head MRI scan, the efficacy of the drug in inhibiting growth of residual pituitary tumor.

Discussion

PKA is an enzyme that plays a central role in the cAMP signal transduction pathway. PKA is activated by cAMP produced by adenylate cyclase through G protein on the plasma membrane. It is believed that PKA predominantly phosphorylates Ser-133 of cAMP response element binding protein (CREB) and subsequently regulates the expression of downstream genes with cAMP response element (CRE). Activation of the cAMP signal transduction pathway by a mutation of Gsα is observed in 30%–50% of patients with sporadic growth hormone-producing pituitary adenoma [10]. The same change is also reported in adrenal adenoma patients. Thus, the activation of downstream genes with CRE through phosphorylation of CREB by PKA is an important factor in the pathogenesis of these endocrine tumors [11]. A mutation of *PRKAR1A* can result in the activation of a downstream gene with CRE by increased activity of PKA. In addition, recent reports suggest associations of *PRKAR1A* with other intracellular signal transduction pathways, such as the suppression of Akt [12] and activation of mTOR [13].

Analyses using knock-out mice have shown that mice deficient in the regulatory subunit *PRKAR1B* protein or homozygous 2A/2B-deficient mice have only mild functional disorders, while homozygous *PRKAR1A*-deficient mice are embryonic lethal. The facts that the homozygous *PRKAR1A*-deficient mice exhibit increased activity of PKA and that these mice show growth impairment and heart defects indicate that the suppressive regulation of PKA by *PRKAR1A* protein is crucial during fetal life [7,14].

Although heterozygous *PRKAR1A*-deficient mice show a normal phenotype, the male animals have a spermatogenic defect and develop carcinomas in various tissues, such as hemangiosarcoma in the spleen, findings similar to those observed in patients with Carney complex. The expression of RIα protein in tumor cells

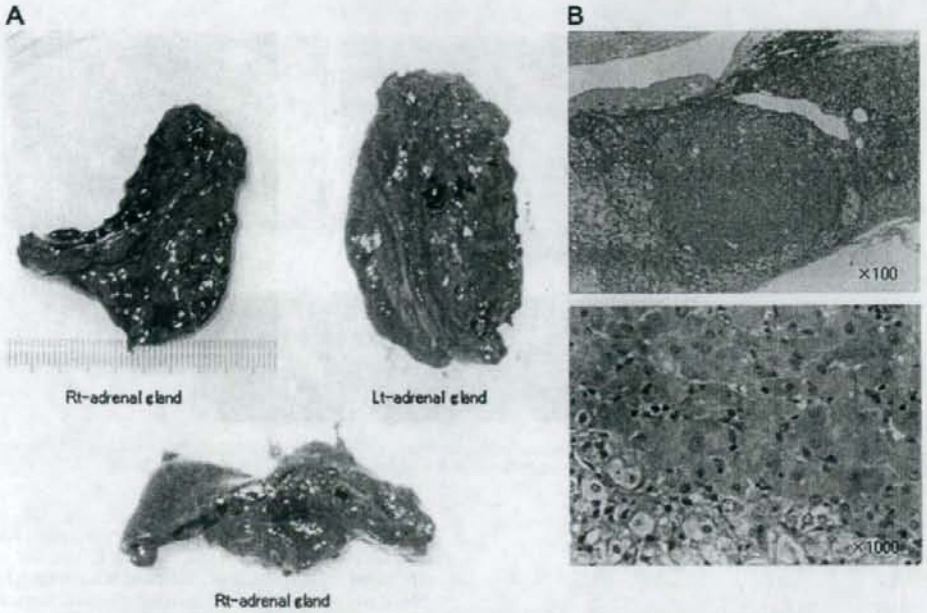

Fig. 4. Pathological findings in adrenal glands of the proband. (A) Macroscopic: Variable sized nodules with black pigmentation were found in bilateral adrenal glands. (B) Microscopic: Severe atrophy was found in zona fasciculate, and nodules comprising eosinophilic cells were observed in zona reticularis. Lipofusutin deposition and adipocyte proliferation were also found.

that developed in these mice suggests the involvement of haploinsufficiency of *PRKAR1A* in the neoplastic process [14]. *PRKAR1A*-inactivating mutations have been identified in more than 150 patients with Carney complex so far. Most of the mutations in *PRKAR1A* result in premature stop codons, and the predicted mutant protein products could not be found in affected cells secondary to nonsense mRNA-mediated decay of the mutant sequence (NMD) [9]. However, there is a report demonstrating that a missense mutation of *PRKAR1A* (R74C) found in patients with the syndrome does cause impairment in the regulation of PKA activity in an *in vitro* system, suggesting the possibility that mechanisms other than haploinsufficiency are involved [15]. It is also known that the impact of PKA activity on cell proliferation varies depending on cell type. For example, increased PKA activity in vascular smooth muscle cells leads to inhibition of cell proliferation. It is thus necessary to clarify the cell- or tissue-specific involvement of PKA in cell proliferation to elucidate the mechanism of the syndrome in the future [16,17].

Table 4
Laboratory data related to adrenal glands in the proband's mother and older sister post the Hardy operation

		99		03.12		04.6	
(A) proband's mother							
ACTH (pmol/l)		10.3		6.3			
Cortisol (nmol/l)				273.1		292.5	
DHEA-S (μmol/l)				1.2		1.1	
GH (μg/l)		8.72		8.36		6.69	
IGF-I (ng/ml)		380		290		270	
	01	04.1	04.8	05.4	06.5	07.7	08.2
(B) Proband's older sister							
ACTH (pmol/l)	1.8	<1.1	1.4	1.3	<1.1	<1.1	
Cortisol (nmol/l)		598.7	179.3	138.0	179.3	298	325.6
DHEA-S (μmol/l)		0.68	0.57	0.35	0.55	0.68	
GH (μg/l)	17.3	29.3	58.6	18.0	21.7	21.5	21.0
IGF-I (ng/ml)	700	710	630	610	541	652	586
PAC (pmol/l)			169.2	66.6		42.2	
PRA (ng/l/s)						0.22	

Mutations in *PRKAR1A* are present in approximately 70% of the patients with Carney complex that have been reported previously, although the mutation c.597delC found in our present patient has not been previously reported. Studies involving a large number of patients report myxoma and pigmentation as characteristic findings of Carney syndrome. However, our patient only showed mild pigmentation and has not shown myxoma at this time by echocardiography (Fig. 5). While only a small number of incidences of PPNAD combined with evident acromegaly are observed, studies involving autopsied patients have reported that pathological changes in the adrenal glands and other organs are found in most patients, indicating that many patients with abnormal findings that can only be diagnosed by endocrinological tests have been overlooked. Indeed, in the present study, if the third sister had not been admitted to hospital and diagnosed with Carney complex, the disease in her mother and sister might well not have been diagnosed. In addition, even family members with the same mutation show distinct phenotypes. Our genetic diagnosis demonstrates that Carney complex is a multifactorial disorder comprising many genetic and environmental factors. In this case, genetic diagnosis played an essential role in determining the appropriateness of bilateral adrenalectomy for treatment of the proband. Genetic diagnosis also was essential in choosing treatment of somatostatin analogue injection for the elder sister, which decreased the cAMP level in cytosol by inhibiting adenylate cyclase, necrotizing her residual pituitary gland.

Genetic diagnosis makes it possible to present clearer therapeutic strategies for treatment during the clinical course for patients and gene carriers and avoid unnecessary tests for non-carriers in the family of the patient.

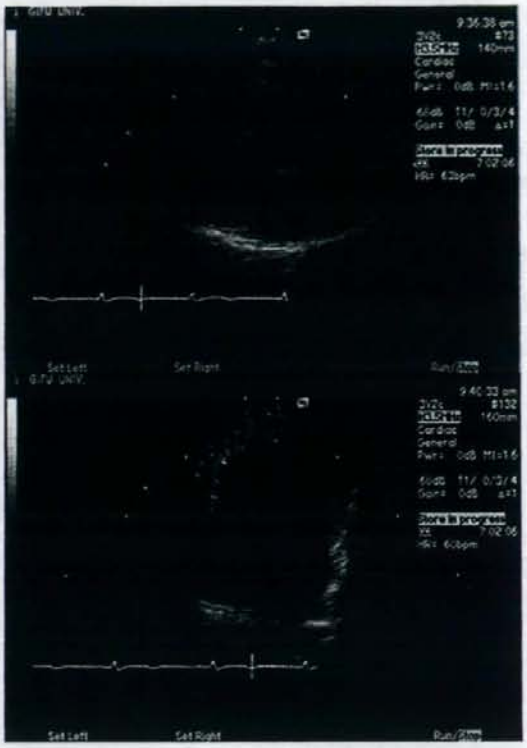

Fig. 5. Ultrasonic cardiogram of the proband.

Acknowledgments

We thank the patient and family for their kind contribution to this report. We thank K. Yokoyama, and H. Tsuchida for technical assistance.

References

[1] J.A. Carney, H. Gordon, P.C. Carpenter, B.V. Shenoy, V.L. Go, The complex of myxomas, spotty pigmentation, and endocrine overactivity, Medicine (Baltimore) 64 (1985) 270–283.

[2] L.S. Kirschner, J.A. Carney, S.D. Pack, S.E. Taymans, C. Giatzakis, Y.S. Cho, Y.S. Cho-Chung, C.A. Stratakis, Mutations of the gene encoding the protein kinase A type I-alpha regulatory subunit in patients with the Carney complex, Nat. Genet. 26 (2000) 89–92.

[3] C.A. Stratakis, L.S. Kirschner, J.A. Carney, Clinical and molecular features of the Carney complex: diagnostic criteria and recommendations for patient evaluation, J. Clin. Endocrinol. Metab. 86 (2001) 4041–4046.

[4] C.A. Stratakis, J.A. Carney, J.P. Lin, D.A. Papanicolaou, M. Karl, D.L. Kastner, E. Pras, G.P. Chrousos, Carney complex, a familial multiple neoplasia and lentiginosis syndrome. Analysis of 11 kindreds and linkage to the short arm of chromosome 2, J. Clin. Invest. 97 (1996) 699–705.

[5] M. Casey, C. Mah, A.D. Merliss, L.S. Kirschner, S.E. Taymans, A.E. Denio, B. Korf, A.D. Irvine, A. Hughes, J.A. Carney, C.A. Stratakis, C.T. Basson, Identification of a novel genetic locus for familial cardiac myxomas and Carney complex, Circulation 98 (1998) 2560–2566.

[6] A. Horvath, S. Boikos, C. Giatzakis, A. Robinson-White, L. Groussin, K.J. Griffin, E. Stein, E. Levine, G. Delimpasi, H.P. Hsiao, M. Keil, S. Heyerdahl, L. Matyakhina, R. Libè, A. Fratticci, L.S. Kirschner, K. Cramer, R.C. Gaillard, X. Bertagna, J.A. Carney, J. Bertherat, I. Bossis, C.A. Stratakis, A genome-wide scan identifies mutations in the gene encoding phosphodiesterase 11A4 (PDE11A) in individuals with adrenocortical hyperplasia, Nat. Genet. 38 (2006) 794–800.

[7] I. Bossis, A. Voutetakis, T. Bei, F. Sandrini, K.J. Griffin, C.A. Stratakis, Protein kinase A and its role in human neoplasia: the Carney complex paradigm Endocrine-related, Cancer 11 (2004) 265–280.

[8] I. Bossis, C.A. Stratakis, Minireview: PRKAR1A: Normal and abnormal functions, Endocrinology 145 (2004) 5452–5458.

[9] S.A. Boikos, C.A. Stratakis, Carney complex: the first 20 years, Curr. Opin. Oncol. 19 (2007) 24–29.

[10] S.A. Boikos, C.A. Stratakis, Molecular genetics of the cAMP-dependent protein kinase pathway and of sporadic pituitary tumorigenesis, Hum. Mol. Genet. 16 (2007) R80–R87.

[11] D. Rosenberg, L. Groussin, E. Jullian, K. Perlemoine, X. Bertagna, J. Bertherat, Role of the PKA-regulated transcription factor CREB in development and tumorigenesis of endocrine tissues, Ann. NY Acad. Sci. 968 (2002) 65–74.

[12] A. Robinson-White, E. Meoli, S. Stergiopoulos, A. Horvath, S. Boikos, I. Bossis, C.A. Stratakis, PRKAR1A Mutations and Protein Kinase A Interactions with Other Signaling Pathways in the Adrenal Cortex, J. Clin. Endocrinol. Metab. 91 (2006) 2380–2388.

[13] M. Mavrakis, J. Lipincott-Schwartz, C.A. Stratakis, I. Bossis, Depletion of type IA regulatory subunit (RI alpha) of protein kinase A (PKA) in mammalian cells and tissues activates mTOR and causes autophagic deficiency, Hum. Mol. Genet. 15 (2006) 2962–2971.

[14] M. Veugelers, D. Wilkes, K. Burton, D.A. McDermott, Y. Song, M.M. Goldstein, K. La Perle, C.J. Vaughan, A. O'Hagan, K.R. Bennett, B.J. Meyer, E. Legius, M. Karttunen, R. Norio, H. Kaariainen, M. Lavyne, J.P. Neau, G. Richter, K. Kirali, A. Farnsworth, K. Stapleton, P. Morelli, Y. Takanashi, J.S. Bamforth, F. Eitelberger, I. Noszian, W. Manfroi, J. Powers, Y. Mochizuki, T. Imai, G.T. Ko, D.A. Driscoll, E. Goldmuntz, J.M. Edelberg, A. Collins, D. Eccles, A.D. Irvine, G.S. McKnight, C.T. Basson, Comparative PRKAR1A genotype-phenotype analysis in humans with Carney complex and prkar1a haploinsufficient mice, Proc. Natl. Acad. USA 101 (2004) 14222–14227.

[15] E.L. Greene, A.D. Horvath, M. Nesterova, C. Giatzakis, I. Bossis, C.A. Stratakis, In vitro functional studies of naturally occurring pathogenic PRKAR1A mutations that are not subject to nonsense mRNA decay, Hum. Mutat. 29 (2008) 633–639.

[16] D. Wilkes, K. Charitakis, C.T. Basson, Inherited disposition to cardiac myxoma development, Nat. Rev. Cancer. 6 (2006) 157–165.

[17] D. Wilkes, D.A. McDermott, C.T. Basson, Clinical phenotypes and molecular genetic mechanisms of Carney complex, Lancet Oncol. 6 (2005) 501–508.

Biochemical and Biophysical Research Communications 374 (2008) 95–100

Contents lists available at ScienceDirect

Biochemical and Biophysical Research Communications

journal homepage: www.elsevier.com/locate/ybbrc

Regulation of lipogenesis via BHLHB2/DEC1 and ChREBP feedback looping

Katsumi Iizuka [a], Yukio Horikawa [a,b,*]

[a] Laboratory of Medical Genomics, The Institute for Molecular and Cellular Regulation, Gunma University, Maebashi-shi Gunma 371-8512, Japan
[b] Department of Diabetes and Endocrinology, Division of Molecule and Structure, Gifu University Graduate School of Medicine, 1-1 Yanagido, Gifu-shi, Gifu 501-1194, Japan

ARTICLE INFO

Article history:
Received 25 June 2008
Available online 9 July 2008

Keywords:
ChREBP
BHLHB2
DEC1
STRA13
Lipogenesis
Carbohydrate response element (ChoRE)

ABSTRACT

BHLHB2/DEC1 is a transcription factor implicated in cell proliferation, apoptosis, and metabolism, and is also known to play an important role in the regulation of the mammalian circadian rhythm. However, its precise role in metabolism remains unclear. We investigated the link between BHLHB2 and ChREBP, a glucose-activated transcription factor involved in the regulation of lipogenesis. Glucose stimulation and overexpression of dominant active ChREBP induced *Bhlhb2* mRNA expression in rat hepatocytes. Deletion studies showed that ChoRE (−160 to −143 bp) in the mouse *Bhlhb2* promoter region is functional in vivo. Overexpression of BHLHB2 inhibited glucose and ChREBP-mediated induction of rat *Fasn* and liver pyruvate kinase (*Lpk*) mRNA. ChIP assay demonstrated that BHLHB2 bound to ChoRE in the *Fasn*, *Lpk*, and *Bhlhb2* promoter regions in vivo. In conclusion, BHLHB2 and ChREBP constitute a novel feedback loop involved in the regulation of lipogenesis.

Excess carbohydrate intake leads to fat accumulation, insulin resistance, and development of metabolic syndrome. Glucose and insulin coordinately regulate de novo lipogenesis in the liver [1]. Insulin regulates lipogenic enzymes and gene expression by the activation of several transcription factors such as sterol regulating element binding protein 1c (SREBP1c) [2]. Glucose also activates lipogenic gene expression by activating the carbohydrate response element binding protein (ChREBP) [1]. ChREBP and Mlx form a heterodimer and bind to the carbohydrate response element (ChoRE) in the promoter of glycolytic and lipogenic enzymes such as liver-type pyruvate kinase (*Lpk*) and fatty acid synthase (*Fasn*) [3,4].

We previously reported that deletion of the ChREBP gene in *ob/ob* mice decreased obesity, hyperglycemia, and fatty liver [4]; however, there was a high amount of glycogen accumulation and hepatomegaly, indicating the need for an alternative therapy. ChoRE is composed of two E-boxes separated by 5 bp [1]. As basic-helix-loop-helix (Bhlh) transcription factors can bind to the E-box, we hypothesized that some of these transcription factors might compete with ChREBP for binding to ChoRE, thereby antagonizing ChREBP transcriptional activity. Therefore, among the transcription factors bound to the E-box, we focused on the transcription repressor basic helix-loop-helix binding Protein 2 (BHLHB2).

BHLHB2 (DEC1 or STRA13) encodes a deduced 412-amino acid protein containing a basic helix-loop-helix (BHLH) domain [5]. BHLHB2 represents a large and diverse class of transcription factors implicated in cell proliferation, apoptosis, and metabolism [5], and is known to play an important role in the regulation of the mammalian circadian rhythm [6]. BHLHB2 and BHLHB3 are helix-loop-helix transcription factors that repress Clock/BMAL1-induced trans-activation of the mouse *Per1* promoter through direct protein–protein interactions with Bmal1 and/or competition for E-box elements [6]. Recently, deletion of the *Clock* gene was reported to cause metabolic syndrome [7], and *Bhlhb2* mRNA was reported to be increased in muscles of diabetic and insulin-resistant humans [8]. These findings suggest that *Bhlhb2* plays an important role in the development of metabolic syndrome.

In this study, we show that glucose induces *Bhlhb2* gene expression through ChREBP activation. Moreover, in rat hepatocytes, overexpression of BHLHB2 inhibits the expression of glucose-induced lipogenic genes by inhibiting the binding of CHREBP to the carbohydrate response element (ChoRE). Thus, this study helps to clarify the relationship between ChREBP and BHLHB2 in glucose regulation, lipid metabolism, and the pathology of metabolic syndrome.

Materials and methods

Animals, isolation of rat primary hepatocytes, and cell culture. The protocols for all animal experiments were approved by the Institutional Animal Care and Use Committee of Gunma University Medical School (code no. 08–025). Rat primary hepatocytes were isolated from 6-week-old male Wister rats by the collagenase perfusion methods [4]. Isolated hepatocytes were suspended with DMEM supplemented with 10% fetal calf serum (FCS), 100 nM insulin, 100 nM dexamethasone (dex), 10 nM triiodothronine (T_3), and 100 μg/ml penicillin/streptomycin (pen/strep). Cells were seeded

* Corresponding author. Address: Department of Diabetes and Endocrinology, Division of Molecule and Structure, Gifu University Graduate School of Medicine, 1-1 Yanagido, Gifu-shi, Gifu 501-1194, Japan. Fax: +81 58 230 6376.
E-mail address: yhorikaw@gifu-u.ac.jp (Y. Horikawa).

0006-291X/$ - see front matter © 2008 Elsevier Inc. All rights reserved.
doi:10.1016/j.bbrc.2008.06.101

in 6-well plates or 10-cm dishes and grown in a humidified atmosphere of 5% CO_2 and 95% air at 37 °C. After the cells were incubated for 4 h, the media was removed and exchanged into DMEM containing 10 nM T_3.

Construction of plasmid and adenovirus vectors. PCR was performed using Prime star DNA polymerase (Takara) and Primers (Sigma–Aldrich). Rat FLAG-tagged dominant active ChREBP deleting 1–196 amino acids (daChREBP) and mouse FLAG-tagged BHLHB2 full length cDNA were amplified from rat and mouse liver cDNA [9]. The nucleotide sequences of PCR primers are shown in Table 1. These PCR fragments were cloned into the pENTR vector (Invitrogen) to produce pENTR-daChREBP and pENTR-BHLHB2. The adenovirus vectors bearing BHLHB2 and daChREBP cDNA were constructed to recombine pENTR-daChREBP or pENTR-BHLHB2 vectors into pAd/CMV/V5-DEST using the LR Clonase II master mix (Invitrogen) according to manufacturer's protocol. The pcDNA6.2 vectors bearing BHLHB2 cDNA (pcDNA-BHLHB2) and daChREBP cDNA (pcDNA-daChREBP) were constructed in the same manner as the adenovirus. The series of 5′-deletions in *Bhlhb2* promoter, termed −1088, −174, −138, and −78 bp vectors were inserted into the pGL3 basic vector (Promega). These promoter fragments were amplified using PCR primer (−1088 F, −174 F, −138 F, −78 F and -R) and Ex Taq DNA polymerase (Takara) (Table 1). The PCR products were digested with HindIII and ligated with pGL3 basic vectors precut by Hind III. The reporter vectors, pGL3-*Fasn* and pGL3-*Lpk*, were the same vectors as used previously [3]. pGL4.74[hRLuc/TK] was purchased from Promega. pGL3 promoter vector was digested with MluI and BglII and dephosphorylated with calf intestinal alkaline phosphatase (Takara). Two oligonucleotides of BHLHB2 (3XChoRE) were denatured at 90 °C for 10 min and annealed at room temperature for 1 h (Table 1). These double stranded oligonucleotides were ligated into the pGL3 promoter vector predigested by MluI and BglII.

Table 1
Oligonucleotide sequences for PCR primers and double stranded DNA inserted into pGL3 promoter vector

Gene name		Nucleotide sequences
DaChREBP (flag)	F	5′-CACCATGGATTACAAGGATGACGACGATAAGATCAGGGA AGGGGATTTCCTGGCTCCCAAGC-3′
	R	5′-TTATAATGGTCTGCCCAGGGGACCCTCTGTG-3′
BHLHB2 (flag)	F	5′-CACCATGGATTACAAGGATGACGACGATAAGATCGAACG GATCCCCAGCGCGCAACC -3′
	R	5′-TTAGTCTTTGGTTTCTAAGT-3′
BHLHB2 promoter	−1088 bp F	5′-gcaagcttTGCAAGTGAGCCGAGCTCCGGCCCG-3′
	−174 bp F	5′-gcaagcttCACTTCGCAGCCGCCAGAGCG-3′
	−138 bp F	5′-gcaagcttGGGAGGGCGGGCAGGTCG-3′
	−78 bp F	5′-gcaagcttACCCACTCGCTCCCATTTAACCC-3′
	R	5′-CGCCGTGCGAGCCAAGTGAAT-3′
BHLHB2 (3XChoRE)	F	5′-CGCGGTCCAACACGTGAGGCTCATGTGATGAAGGTCCAA CACGTGAGGCTCATGTGATGAAGGTCCAACACGTGAGGCTC ATGTGATGAAG-3
	R	5′-GATCCTTCATCACATGAGCCTCACGTGTTGGACCTTCATC ACATGAGCCTCACGTGTTGGACCTTCATCACATGAGCCTCAC GTGTTGGAC-3′
LPK for ChIP	F	5′-CTTTGATCCGAGGCTCTGCAGAC-3′
	R	5′-TGAGTCCTGGTTAAAGTATAACC-3′
BHLHB2 for ChIP	F	5′-GCAGCCGCAGACACCTGGGGCCCGAGG-3′
	R	5′-CGTGTTCTACCCTGTGACTCCAAGCAC-3′
FASN for ChIP	F	5′-AAAGGCCTGCTCTGGAATCATTCTC-3′
	R	5′-CAGAGAGGCTTGCTGAAGCTGAGACC-3′

Mammalian transfection and Reporter assay. Primary hepatocytes were cultured in 6 plates in 2 ml DMEM medium without anibiotics. After 20 multiplicity of infection (m.o.i.) of adenovirus bearing GFP, BHLHB2 or daChREBP cDNA was infected into the hepatocytes for 2 h, and the cells were transfected with lipofectamine2000 (10 μl), pGL3-*Fasn*, or -*Lpk* (3.6 μg), or a deletion series of BHLHB2 vectors and the pGL4.74[hRLuc/TK] vector (0.4 μg). After 24 h of incubation, the cells were collected and used to measure luciferase activity (Dual Luciferase assay system; Promega) according to Manufacture's protocol. To measure the effect of BHLHB2 and daCHREBP, cells were cotransfected with the pGL3-*Fasn* or -*Lpk* vector (3.0 μg), pGL4.74[hRLuc/TK] vector (0.4 μg), pcDNA-BHLHB2 (0.2 μg), and/or pcDNA-daChREBP (0.2 μg). The total amount of DNA was adjusted by the addition of an empty vector.

RNA isolation and semi-quantitative RT-PCR. Total RNA was isolated using the RNeasy Mini Plus kit (Qiagen) according to the manufacturer's protocol. Single-stranded cDNA was synthesized from the RNA of each sample (0.1 μg), 0.01 mM DTT, 0.5 mM of each dNTP, random primer (0.5 μg), 40 U RNase Out ribonuclease inihibitor, and 200 U SUPERSCRIPT III reverse transcriptase (Invitrogen). The resulting cDNA products (1 ng), water (5 μl), and PCR master mix (10 μl) were used in the Taqman PCR assay with an ABI prism 7900 sequencing detector (Applied Biosystems) on the cDNA samples. Taqman PCR probes for semi-quantitative RT-PCR were purchased from Applied Biosystems.

Chromatin immunoprecipitation (ChIP) assay. Rat hepatocytes were isolated and cultured in 10-cm culture dishes in DMEM supplemented with 10% FCS, 100 nM insulin, 100 nM dex, 10 nM T_3 and 100 μg/ml pen/strep for 4 h and then for 2 h in DMEM supplemented with 10 nM T_3 and 100 μg/ml pen/strep. After the incubations, 10% formaldehyde (270 μl) was added to the culture dishes and the cells were used in the chromatin immunoprecipitation (ChIP) assay according to the manufacturer's protocol. The purified DNA was dissolved in Tris/EDTA (50 μl, pH 8.0) and used with gene specific primers for the PCR (Table 1). The ChIP assays were performed using anti-Mlx (Santa Cruiz Biotechnology), anti-ChREBP (Cayman Chemical) and anti-FLAG antibody (Sigma–Aldrich). Buffer only and rabbit normal IgG (Wako Chemical) were used as the negative control.

Statistical analyses. Results are reported as means ± SD. The comparison of different groups was carried out using two-tailed unpaired Student's *t* test. Differences were considered statistically significant at $p < 0.05$.

Results

Glucose activation of Bhlhb2 gene expression

Increases in *Bhlhb2* mRNA have been reported for diabetic and insulin-resistant patients, and insulin is known to increase *Bhlhb2* expression [5,8]; however, whether glucose activates *Bhlhb2* expression remains unclear. Mouse, rat, and human proximal *Bhlhb2* promoters contain the conserved ChoRE, which is composed of one perfect E-box and one imperfect E-box, separated by 5-bp spaces (Fig. 1A). *Lpk* and *Fasn* are well known to be glucose-response genes targeted by ChREBP [1].

We therefore used *Lpk* and *Fasn* as positive controls for our experiments. Glucose dose-dependently activated *Bhlhb2* mRNA expression in rat primary hepatocytes, and there was a 2.15-fold increase in *Bhlhb2* mRNA at a glucose concentration of 25 mM compared with that at 0.1 mM glucose (Fig. 1B). Moreover, increases of 2.4-, 1.1-, and 5.3-fold were found in cells treated with insulin alone, high-concentration glucose alone, or in combination, respectively (Fig. 1C). We then constructed a series of deletion mutants of the pGL3-BHLHB2 vectors to test the role of putative ChoRE on glucose-activated *Bhlhb2* expression. Glucose activated only the −1088 and −174 bp vectors, including putative ChoRE (Fig. 1D).

ChREBP regulatation of Bhlhb2 gene expression

ChREBP is activated by glucose and binds to ChoRE of the lipogenic gene promoter region. The ChoRE of mouse *Bbhlhb2* is similar to ChoRE of *Lpk* and *Fasn* [1]. We then tested whether ChREBP regulates mouse *Bhlhb2* mRNA expression by binding directly to ChoRE of the *Bhlhb2* gene promoter. The *Bhlhb2* mRNA level was dose-dependently up-regulated by the overexpression of daChREBP (Fig. 2A). By increasing the dose of adenovirus bearing daChREBP cDNA, ChREBP mRNA was increased 5-, 12-, and 63-fold compared with endogenous ChREBP mRNA. Like *Fasn* and *Lpk*, *Bhlhb2* mRNA was also increased 2.1-fold. To test whether daChREBP could directly activate mouse *Bhlhb2* gene promoter, we ran the reporter assay against the series of deleted pGL3-Bhlhb2 vectors (−1088, −174, −138, −78 bp) (Fig. 1D). Overexpression of daChREBP increased the transactivity of −1088 and −174, which contain putative ChoRE (Fig. 2B). We also used pGL3 promoter vectors containing tandem 3XChoRE (from −166 to −138 bp) and tested whether a putative ChoRE possessed glucose responsiveness. The luciferase activity at a glucose concentration of 25 mM was 2-fold higher than that of the control cells (Fig. 2C) and the daChREBP overexpression was 18-fold higher than that in the control cells; however, BHLHB2 alone potently inhibited reporter activity to one-tenth the level of the control cells. Thus, ChoRE in *Bhlhb2* gene promoter possessed glucose responsiveness. Consistent with these data, the ChIP assay showed that ChREBP and Mlx bound to ChoRE of mouse *Bhlhb2* and *Lpk* (Fig. 2D).

BHLHB2 antagonizes the effect of ChREBP on the transactivities of LPK and FAS promoter

BHLHB2 is known to be a transcriptional repressor of gene expression by binding to the E-box (consensus sequence: CACGTG) in the promoter region. ChoRE is composed of two E-boxes separated by a 5-bp insert. We then examined the role of BHLHB2 in glucose activation of lipogenic gene expression. Adenoviral overexpression of BHLHB2 cDNA dose-dependently suppressed glucose-induced mRNA expression of *Fasn* and *Lpk* (Fig. 3A). Interestingly, the inhibitory effect of BHLHB2 on the *Fasn* gene was more potent than that on *Lpk*, probably due to

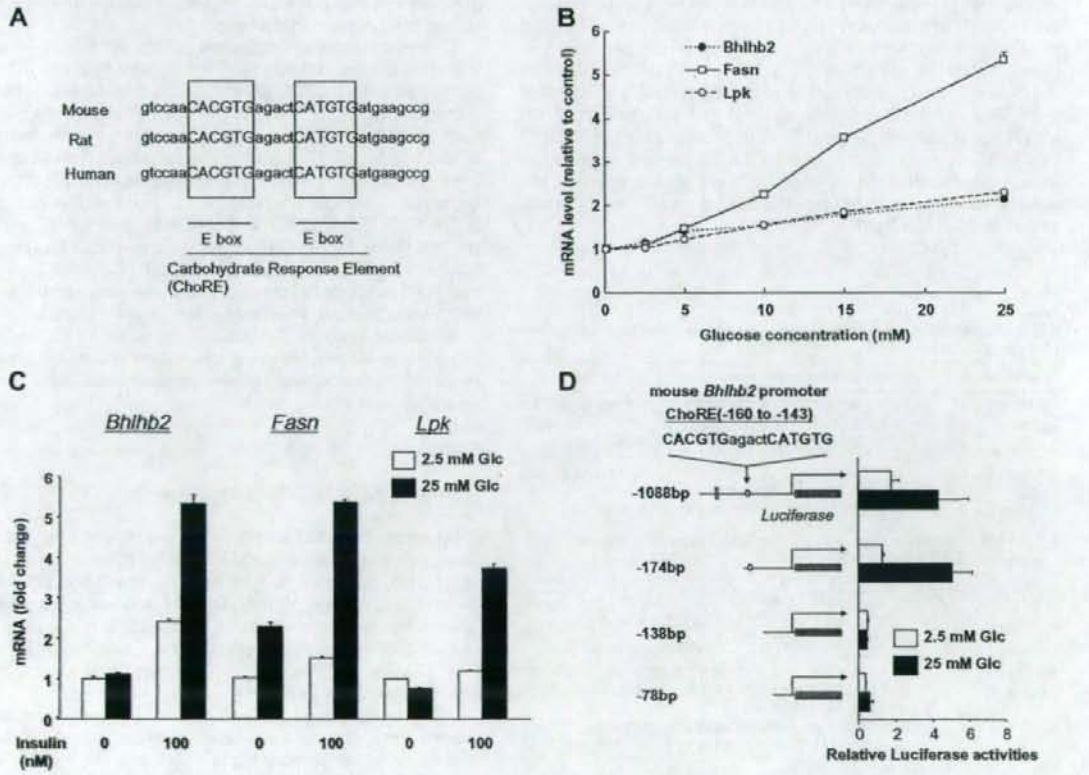

Fig. 1. Regulation of the mouse *Bhlhb2* promoter by glucose in rat primary hepatocytes. (A) A schematic representation of the mouse Bhlhb2 promoter with the sequences and locations of the carbohydrate response element (ChoRE). (B) Dose-dependent effects of glucose on *Bhlhb2*, *Fasn*, and *Lpk* mRNA expression in rat primary hepatocytes. Primary hepatocytes isolated from 6-week-old male Wister rats were cultured for 18 h in culture medium containing 0.1, 2.5, 5.0, 10, 15, or 25 mM glucose. Relative mRNA levels were determined by real-time RT-PCR and normalized to rat RNA polymerase II (*Pol2*) mRNA as the invariant control. The -fold change in expression level of each normalized enzyme mRNA level was determined with reference to the value for hepatocytes at 0.1 mM glucose, which was arbitrarily defined as 1. (C) Synergistic effects of glucose and insulin on *Bhlhb2*, *Fasn*, *and Lpk* mRNA expression. Rat hepatocytes were incubated for an additional 18 h in serum-free culture medium containing either a low (2.5 mM, open bars) or high (25 mM, filled bars) glucose (Glc) concentration in the absence or presence (100 nM) of insulin. (D) A schematic representation of the mouse Bhlhb2 promoter luciferase deletion constructs and the effect of these deletions on relative luciferase activity with low (2.5 mM) or high (25 mM) Glc concentration. Various reporter gene plasmids (−1088, −174, −138, and −78 bp) were cotransfected into rat hepatocytes with pGL4.74[hRluc/TK] as a reference, and luciferase activity was normalized to *Renilla* luciferase activity. The values are represented as means and SD ($n = 6$). The figure represents data from two independent experiments.

the difference of nucleotide sequence in ChoRE. At 25 mM glucose, cotransfection of BHLHB2 suppressed luciferase activity of the *Fasn* and *Lpk* promoters (Fig. 3B). Moreover, BHLHB2 antagonized ChREBP-mediated *Fasn* and *Lpk* promoter activities in rat hepatocytes (Fig. 3C). The ChIP assay showed that BHLHB2 bound ChoRE in the promoter region of *Fasn*, *Lpk*, and the *Bhlhb2* gene (Fig. 3D). Thus, BHLHB2 antagonized ChREBP-mediated lipogenic gene expression by competing for binding to the E-box (Fig. 3E).

Discussion

In this study, we show that the glucose-activated transcription factor, ChREBP, regulates mouse *Bhlhb2* gene expression by directly binding to ChoRE in the mouse *Bhlhb2* promoter. BHLHB2 competes with ChREBP for binding to ChoRE and suppresses the transactivities of *Fasn*, *Lpk*, *and Bhlhb2* promoter mediated by ChREBP. These data indicate that BHLHB2 and ChREBP coordinately regulate de novo lipogenesis in the rat liver.

We also show that CHREBP induces *Bhlhb2* mRNA expression by binding to ChoRE in the *Bhlhb2* promoter region. In the presence of insulin, glucose is converted to Xu-5-P, a metabolite of the pentose phosphate pathway, and activates protein phosphatase 2A and ChREBP by dephospohorylation of the ChREBP protein [1]. In the absence of insulin, glucose was not metabolized into Xu-5-P, and did not activate ChREBP. Consistent with these results, glucose alone did not induce *Bhlhb2* mRNA (Fig. 1C). Moreover, 25 mM xylitol, which is immediately converted to Xu-5-P, induced a 6.4-fold increase *Bhlhb2* mRNA in rat hepatocytes (data not shown). These results indicate that glucose and Xu-5-P induce *Bhlhb2* mRNA expression. Previous studies have reported that *Bhlhb2* mRNA levels in the liver are suppressed during fasting and induced 36 h later during refeeding [10]. These results indicate that *Bhlhb2* expression is regulated by glucose both in vitro and in vivo.

Mouse, rat, and humans share the same ChoRE in the Dec1 promoter region (Fig. 1A). According to the deletion studies of the reporter assay, ChoRE in the *Bhlhb2* promoter region is required for ChREBP-mediated induction of this gene. Moreover, ChREBP

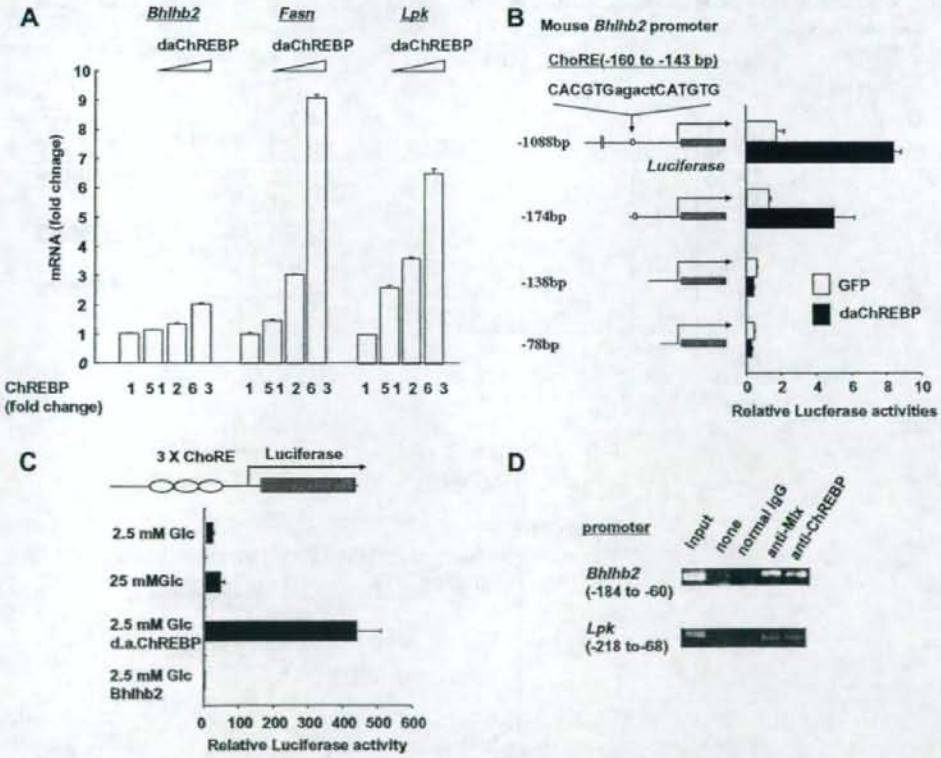

Fig. 2. Regulation of the mouse *Bhlhb2* promoter by ChREBP in rat primary hepatocytes. (A) Adenoviral overexpression of daChREBP activates mouse *Bhlhb2* mRNA expression. In hepatocytes infected with 5, 20, and 50 m.o.i. of Ad daChREBP or 50 m.o.i. of Ad-GFP, ChREBP mRNA was increased 5-, 12-, and 63-fold, respectively. The ChREBP, *Bhlhb2*, *Fasn*, *and LPK* mRNA levels were analyzed by Taqman RT-PCR and corrected with pol2. Data are means and SD. (n = 3) of two independent experiments. (B) A schematic representation of mouse *Bhlhb2* promoter luciferase deletion constructs and the effect of these deletions on relative lucieferase activity with overexpression of daChREBP. Various pGL3 plasmids (−1088, −174, −138, and −78 bp,) were cotransfected into rat hepatocytes with pGL4.74[hRLuc/TK] as a reference. The luciferase activity was normalized to *Renilla* luciferase activity. Data are the means ± SD (n = 6) of two independent experiments. (C) Putative ChoRE in the mouse *Bhlhb2* gene is a response element activated by glucose and ChREBP. The pGL3 promoter vector containing tandem 3X BHLHB2 ChoRE was cotransfected into rat primary hepatocytes with the pGL4.74[hRLuc/TK], pcDNA6.2-daCHREBP vector, and/or pcDNA6.2-BHLHB2 vector. Total DNA was adjusted with pcDNA 6.2 empty vectors. The relative luciferase activity was expressed as -fold change with reference to the pcDNA6.2 empty vector. Data are the means ± SD (n = 6) of two independent experiments. (D) Cells were incubated for 4 h in media and subjected to chromatin immunoprecipitation assay (CHIP assay) using the anti-ChREBP or Mlx antibody. Buffer alone and non-specific rabbit IgG were used as the negative control. Immunoprecipitated samples were subjected to PCR using primers to amplify ChoRE containing regions of the rat *Bhlhb2* or *Lpk* promoters. All experiments were performed in duplicate.

directly bound to ChoRE in the mouse *Bhlhb2* promoter, and overexpression of ChREBP increased *Bhlhb2* mRNA. Some groups have reported that USF2 binding to ChoRE prevents activation of the rat *Bhlhb2* promoter [11]. As with the *Bhlhb2* gene promoter, when USF bound to ChoRE in the *Fasn* and *Lpk* promoters, it did not induce expression of these genes [12]. SREBP1c belongs to the bHLH transcription factor family and binds to their E-box in vitro [2]. While insulin induces *Bhlhb2* expression, the precise mechanism is unclear. In preliminary data, a 20-fold increase in the overexpression of SREBP1c increased *Bhlhb2* mRNA 6-fold in mouse

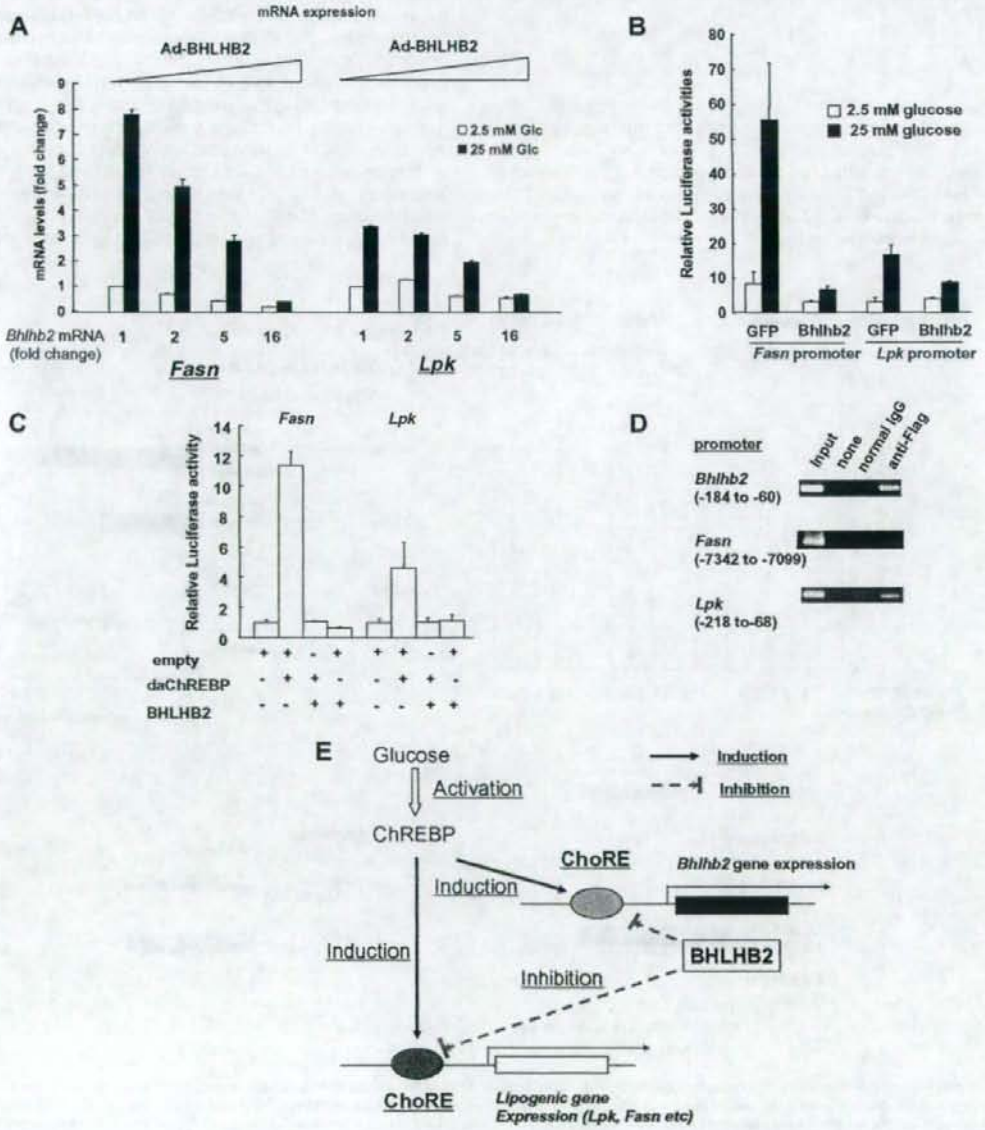

Fig. 3. Bhlhb2 antagonizes the effect of ChREBP on the transactivities of the *Lpk* and *Fasn* promoter. (A) Bhlhb2 dose-dependently inhibited glucose-induced gene expression in rat primary hepatocytes. In hepatocytes infected with 5, 20, or 50 m.o.i. of Ad-BHLHB2 and Ad-GFP adenovirus, *Bhlhb2* mRNA increased 5-, 12-, and 63-fold, respectively. *Fasn* and *Lpk* mRNA levels were detected by Taqman RT-PCR and corrected with pol2 mRNA. Data are represented as means and SD. (B) Overexpression of *Bhlhb2* antagonized glucose-mediated *Fasn* and *Lpk* promoter activities in rat hepatocytes. pGL3-*Fas* or -*Lpk* and pGL4.74[hRLuc/TK] was cotransfecetd into rat primary hepatocytes infected with 50 m.o.i. of Ad GFP or BHLHB2. (C) BHLHB2 inhibited ChREBP-mediated transcription activities in *Fasn* and *Lpk* promoters. pGL3 *Fasn* or *Lpk* and pGL4.74[hRLuc/TK] was cotransfected into hepatocytes with pcDNA-BHLHB2 and/or pcDNA-daChREBP. (D) Rat hepatocytes overexpressing BHLHB2 cDNA were subjected to ChIP assay with an anti-FLAG monoclonal antibody and rabbit IgG as the negative control. Immunoprecipitated samples were subjected to PCR analysis using primers to amplify ChoREs in the *Lpk*, *Fas*, and *Bhlhb2* promoter. (E) A schematic representation of the feedback loop model for the de novo coordinate regulation of lipogenesise in rat hepatocytes by ChREBP and BHLHB2.

hepatocytes. Further investigation is required to determine whether SREBP1c induces *Bhlhb2* mRNA by binding to ChoRE and the E-box. These results indicate that ChREBP regulates *Bhlhb2* expression by binding to ChoRE in the promoter region of the *Bhlhb2* gene.

We have shown that BHLHB2 inhibits glucose- and ChREBP-mediated lipogenic gene expression in rat hepatocytes. ChREBP transactivity is known to be partly regulated by a phosphorylation/dephosphorylation mechanism, although the details remain unclear [1]. We show here that the link between ChREBP and BHLHB is a novel feedback loop involved in the regulation of lipogenesis (Fig. 3E). A similar feedback system is also seen between BHLHB2 and Clock/BMAL. The Clock/BMAL1 complex recognizes the perfect E-box in ChoRE of the *Bhlhb2* promoter region, and induces *Bhlhb2* mRNA expression [6]. In contrast, BHLHB2 is a transcriptional repressor that binds to the E-box in the promoter region of *Per1* and *Bhlhb2*, and represses the gene induction mediated by Clock/BMAL1. Thus, a negative feedback loop between BHLHB2 and Clock/BMAL1 is involved in the regulation of the circadian rhythm [6]. Based on these results, we tested the hypothesis that ChREBP and BHLHB2 compete for binding to the *Fasn* and *Lpk* promoters of ChoRE to form a negative feedback loop that regulates lipogenesis. The results of our ChIP and reporter assays supportes this hypothesis. BHLHB2 has also been shown to bind to ChoRE at the *Bhlhb2* promoter region, potentially inhibiting its promoter activity [13]. Our data also show that overexpression of BHLHb2 inhibits the promoter activity of the pGL3 promoter vector with 3X Bhlhb2 ChoRE in hepatocytes, and that BHLHB2 binds to ChoRE in its promoter. For this reason, while the luciferase activity of PGL3-3XBHLHB2 ChoRE is dramatically induced by ChREBP, the effect of ChREBP on the induction of *Bhlhb2* mRNA may be only modest.

The physiological significance of the negative feedback loop between ChREBP and BHLHB2 remains unclear. In muscles from diabetic patients, *Bhlhb2* mRNA was found to be remarkably increased [8]. Consistent with this data, we found that ob/ob mice and 6-month high fat diet-loaded mice showed *Bhlhb2* mRNA in the liver 4.2 and 3.6 times higher than that in control mice, respectively ($n=4$, $p<0.05$). Moreover, a 6-fold overexpression of BHLHB2 inhibited glucose-mediated induction of *Fasn* and *Lpk* by 40% and 60%, respectively. Thus, the inhibitory effect of BHLHB2 on the FAS gene is probably more important than the inhibition on the *Lpk* gene. Furthermore, the 6-fold overexpression of BHLHB2 potently inhibited ChREBP-mediated induction of *Fasn* and *Lpk* expression. These results indicate that BHLHB2 regulates glucose activation of lipogenic enzyme gene expression and plays an important role in preventing overshoot of ChREBP-mediated lipid synthesis. Analysis of the effect of fasting and refeeding on *Fasn* and *Lpk* mRNA expression in ChREBP and Bhlhb2 knockout mice should permit identification of the physiological role of *Bhlhb2* in glucose-mediated lipogenic gene expression.

In conclusion, we have demonstrated that BHLHB2 is regulated by glucose and ChREBP and that it is inhibited by glucose and ChREBP-mediated *Fasn* and *Lpk* expression. Thus, ChREBP and BHLHB2 constitute a negative feedback loop involved in the regulation of lipogenesis. Further studies to clarify the in vivo relationship between BHLHB2 and ChREBP will be helpful for understanding the mechanism of regulation of lipogenesis and the development of treatments for metabolic syndrome.

Acknowledgments

This work was supported by a Grant in Aid for Scientific Research from the Japan Society for the Promotion of Science (K. Iizuka), the ONO Medical Research Foundation (K. Iizuka) and in part, by a New Energy and Industrial Technology Development Organization grant to Y. Horikawa.

References

[1] K. Iizuka, Y. Horikawa, CHREBP: a glucose activated transcription factor involved in the development of metabolic syndrome, Endocr. J., doi:10.1507/endocrj.K07E-110.
[2] H. Shimano, Sterol regulatory element-binding proteins (SREBPs): transcriptional regulators of lipid synthetic genes, Prog. Lipid Res. 40 (2001) 439–452.
[3] S. Ishii, K. Iizuka, B.C. Miller, K. Uyeda, Carbohydrate response element binding protein directly promotes lipogenic enzyme gene transcription, Proc. Natl. Acad. Sci. USA 101 (2004) 15597–15602.
[4] K. Iizuka, B. Miller, K. Uyeda, Deficiency of carbohydrate-activated transcription factor ChREBP prevents obesity and improves plasma glucose control in leptin-deficient (ob/ob) mice, Am. J. Physiol. Endocrinol. Metab. 291 (2006) E358–E364.
[5] K. Yamada, K. Miyamoto, Basic helix-loop-helix transcription factors, BHLHB2 and BHLHB3; their gene expressions are regulated by multiple extracellular stimuli, Front. Biosci. 10 (2005) 3151–3171.
[6] S. Honma, T. Kawamoto, Y. Takagi, K. Fujimoto, F. Sato, M. Noshiro, Y. Kato, K. Honma, Dec1 and Dec2 are regulators of the mammalian molecular clock, Nature 419 (2002) 841–844.
[7] F.W. Turek, C. Joshu, A. Kohsaka, E. Lin, G. Ivanova, E. McDearmon, A. Laposky, S. Losee-Olson, A. Easton, D.R. Jensen, R.H. Eckel, J.S. Takahashi, J. Bass, Obesity and metabolic syndrome in circadian Clock mutant mice, Science 308 (2005) 1043–1045.
[8] D.K. Coletta, B. Balas, A.O. Chavez, M. Baig, M. Abdul-Ghani, S.R. Kashyap, F. Folli, D. Tripathy, L.J. Mandarino, J.E. Cornell, R.A. Defronzo, C.P. Jenkinson, Effect of acute physiological hyperinsulinemia on gene expression in human skeletal muscle in vivo, Am. J. Physiol. Endocrinol. Metab. 294 (2008) E910–E917.
[9] M.V. Li, B. Chang, M. Imamura, N. Poungvarin, L. Chan, Glucose-dependent trans criptional regulation by an evolutionarily conserved glucose-sensing module, Diabetes 55 (2006) 1179–1189.
[10] T. Kawamoto, M. Noshiro, M. Furukawa, K.K. Honda, A. Nakashima, T. Ueshima, E. Usui, Y. Katsura, K. Fujimoto, S. Honma, K. Honma, T. Hamada, Y. Kato, Effects of fasting and re-feeding on the expression of Dec1, Per1, and other clock-related genes, J. Biochem. 140 (2006) 401–408.
[11] S. Hirano, K. Yamada, H. Kawata, Z. Shou, T. Mizutani, Y. Shigematsu, M. Mayumi, K. Miyamoto, The rat enhancer of split- and hairy-related protein-2 gene: hepatic expression, genomic structure, and promoter analysis, Arch. Biochem. Biophys. 422 (2004) 81–90.
[12] E.N. Kaytor, H. Shih, H.C. Towle, Carbohydrate regulation of hepatic gene expression. Evidence against a role for the upstream stimulatory factor, J. Biol. Chem. 272 (1997) 7525–7531.
[13] T. Kawamoto, M. Noshiro, F. Sato, K. Maemura, N. Takeda, R. Nagai, T. Iwata, K. Fujimoto, M. Furukawa, K. Miyazaki, S. Honma, K. Honma, Y. Kato, A novel autofeedback loop of Dec1 transcription involved in circadian rhythm regulation, Biochem. Biophys. Res. Commun. 313 (2004) 117–124.

Biochemical and Biophysical Research Communications 379 (2009) 499–504

Contents lists available at ScienceDirect

Biochemical and Biophysical Research Communications

journal homepage: www.elsevier.com/locate/ybbrc

Hepatic overexpression of dominant negative Mlx improves metabolic profile in diabetes-prone C57BL/6J mice

Katsumi Iizuka [a], Jun Takeda [b], Yukio Horikawa [a,b,*]

[a] Laboratory of Medical Genomics, The Institute for Molecular and Cellular Regulation, Gunma University, Maebashi-shi, 371-8512, Japan
[b] Department of Diabetes and Endocrinology, Gifu University, Graduate School of Medicine, Gifu, 501-1194, Japan

ARTICLE INFO

Article history:
Received 9 December 2008
Available online 31 December 2008

Keywords:
Mlx
Glucose-6-phosphatase
ChREBP
Metabolic Syndrome
Elovl6
Transketolase

ABSTRACT

Mlx and ChREBP form a heterodimer to regulate glucose-mediated gene expression in the liver. Thi study was performed to determine if the metabolic syndrome might be improved using dominant neg ative Mlx (dnMlx). An adenovirus bearing dnMlx was constructed and used to test the inhibitory effec of dnMlx on lipogenesis both *in vitro* and *in vivo*. Adenoviral overexpression of dnMlx in rat hepatocyte inhibited expression of glucose-regulated genes, including *Chrebp* and *Transketolase*, which constitute positive feedback loop in the regulation of *Chrebp* gene expression. Adenoviral overexpression of dnMl in 25-week-old male C57BL/6J mice reduced hepatic triglyceride contents and improved glucose intoler ance by inhibiting expression of *Glucose-6-phosphatase* and *Elovl6* mRNA in addition to lipogeni enzymes. In conclusion, overexpression of dnMlx improves glucose intolerance by inhibiting expressio not only of lipogenic enzymes but also other important genes such as *Glucose-6-phosphatase* and *Elovl6*

Nonalcoholic fatty liver disease is associated with metabolic syndrome and poses increased risk of cardiovascular disease. Development of non-alcoholic fatty liver disease is caused by decreased fatty acid oxidation and/or increased triglyceride synthesis. In the fed state, excess glucose uptake is converted to liver triglyceride storage. Hepatic *de novo* lipogenesis is regulated by insulin and glucose. Insulin and glucose induces glycolytic and lipogenic gene expression by sterol regulatory element binding protein (SREBP1c) and carbohydrate response element binding protein (ChREBP), respectively, [1,2]. Experiments in knockout mice indicate that SREBP1c and ChREBP exhibit *de novo* lipogenesis of 50% and 60%, respectively, [1]. Inhibition of these transcription factors reverses hepatic steatosis in obesity [1]. Thus, SREBP1c and ChREBP coordinately regulate hepatic lipogenesis. ChREBP heterodimerizes with Mlx to bind to the carbohydrate response elements (ChoRE) in the promoter of glycolytic and lipogenic genes [1].

We previously reported that gene deletion of ChREBP in ob/ob mice improved metabolic syndrome compared with ob/ob mice [3]. Consistent with our previous study, adenoviral delivery of ChREBP short hairpin RNA (shRNA) into the liver improved hepatic steatosis and insulin resistance by inhibiting hepatic lipogenesis [4]. In contrast, liver-specific inhibition of SREBP1c was found to improve hepatic steatosis but not glucose intolerance [1]. Liver specific inhibition of PPARγ also improved hepatic steatosis, but in creased glucose intolerance [1]. Clarification of the differences be tween ChREBP and SREBP1c or PPARγ in the development of th metabolic syndrome thus might facilitate development of clinica treatment options for the condition [1].

In this study, we investigate the mechanism of the improve ment by liver-specific inhibition of ChREBP transactivity of glucos intolerance. An adenovirus bearing dominant negative Ml (dnMlx) was constructed to test the transactivity of ChREB *in vitro* and *in vivo*. Our findings in Ad-dnMlX-injected mice sug gest that drugs disrupting the association between ChREBP an Mlx might be useful in preventing metabolic syndrome.

Materials and methods

Animals, isolation of rat primary hepatocytes, and cell culture. Th protocols for all animal experiments were approved by the Institu tional Animal Care and Use Committee of Gunma University Med ical School (code no. 08-025). Six-week-old male Wistar rats wer purchased from Japan SLC (Hamamatsu, Shizuoka, Japan) and mal C57BL/6J mice were purchased from Charles River Japan (Yoko hama, Kanagawa, Japan). Rat hepatocytes were isolated from 6 week-old male Wistar rats by the collagenase perfusion method Isolated hepatocytes were suspended in DMEM supplemente with 10% fetal calf serum (FCS), 100 nM insulin, 100 nM dex 10 nM T_3, and 100 μg/ml pen/strep [5]. Cells were seeded in 6-wel plates or 10-cm dishes and grown in a humidified atmosphere o

* Corresponding author. Address: Department of Diabetes and Endocrinology, Division of Molecule and Structure, Gifu University School of Medicine, Gifu, Japan. Fax: +81 58 230 6376.
E-mail address: yhorikaw@gifu-u.ac.jp (Y. Horikawa).

0006-291X/$ - see front matter © 2008 Elsevier Inc. All rights reserved.
doi:10.1016/j.bbrc.2008.12.100

5% CO_2/95% air at 37 °C. After incubation for 4 h, the medium was replaced with DMEM containing 10 nM T_3.

Construction of plasmid and adenovirus vectors. PCR to construct pENTR vectors was performed using PrimeSTAR DNA polymerase (Takara) and primers (Sigma–Aldrich). A series of Mlx deletion mutants with an N-terminal Flag tag were amplified from mouse liver cDNA (Fig. 1A). PCR fragments (2–245aa, 67–245aa, and 88–245aa) were cloned into the pENTR vector (Invitrogen), yielding pENTR-Mlx1-1, -Mlx2-1, or -Mlx4-1, respectively. Adenovirus vectors bearing Mlx4-1 were constructed by recombining pENTR-Mlx4-1 vectors into pAd/CMV/V5-DEST using LR Clonase II Master Mix (Invitrogen) according to the manufacturer's protocol. The pcDNA6.2 vectors bearing Mlx1-1, Mlx2-1, or Mlx4-1 (pcDNA-Mlx1-1, pcDNA-Mlx2-1, or pcDNA-Mlx4-1, respectively) were constructed in the same manner as the adenovirus. pGL3-Lpk and Ad-daChREBP were the same vector and adenovirus used previously [5]. pGL4-TK-RLuc vector was purchased from Promega.

Treatment with recombinant adenovirus in rat hepatocytes. Rat isolated hepatocytes were cultured in 6-well plates in 2 ml of DMEM. Hepatocytes were infected with adenovirus bearing GFP, Mlx4-1, or dominant active ChREBP (daChREBP) at m.o.i. of 2, 10, or 50 for 2 h, media were removed, and infected cells were incubated in media with 2.5 or 25 mM glucose for 18 h. The cells were then collected and used for RT-PCR analysis.

RNA extraction and quantitative real-time PCR. Total RNA was extracted from hepatocytes or liver samples using an RNeasy Mini Plus kit (Qiagen) according to the manufacturer's protocol [5]. Taqman PCR probes for semi-quantitative RT-PCR were purchased from Applied Biosystems.

Mammalian transfection and reporter assay. Primary hepatocytes were cultured in 6-well plates in 2 ml of DMEM without antibiotics. The cells were transfected with Lipofectamine 2000 (10 μl), pGL3-Lpk (3.6 μg), or the series of pcDNA-Mlx vectors (empty, Mlx1-1, Mlx2-1, or Mlx4-1) (0.4 μg) and the pGL4-TK-Renilla luciferase vector (0.4 μg) [5]. After 24 h of incubation with 2.5 or 25 mM glucose, the cells were collected and used to measure luciferase activity (Dual Luciferase Assay System; Promega) according to the manufacturer's protocol.

Establishment of Ad dominant negative Mlx4-1-infected mice. Twenty-five-week-old male C57BL/6J mice were anesthetized with pentobarbital and injected *via* the tail vein with 3×10^{13} particle/kg body weight (BW) of Ad-GFP or Ad-Mlx4-1 in a final volume of 300 μl of phosphate buffered saline. After 5 days, the mice were sacrificed and the liver was used for extraction of total RNA and liver metabolites.

Measurement of plasma profile and liver metabolites and oral glucose tolerance test. Plasma concentrations of glucose, insulin, and triglyceride were measured as described previously [3]. Total cholesterol, alanine aminotransferase (ALT), and aspartate aminotransferase (AST) were measured using Cholesterol and Transaminase Wako test kits (Wako). Liver glycogen, triglyceride, and cholesterol contents were measured as described previously [3]. Oral glucose tolerance tests at 3 days were performed by oral injection of glucose at a dose of 1 g glucose/kg BW after 18-h fast. Blood glucose levels were measured at the designated times using a FreeStyle Kissei Meter (Kissei, Tokyo, Japan).

Data presentation and statistical methods. All data are expressed as means ± SD. The listed n values represent the number of single experiments performed (each experiment was duplicated). Comparisons between two groups were performed by Student's t-test, and $P < 0.05$ was considered significant.

Results

Mlx4-1 acts as dominant negative Mlx to inhibit glucose-induced Lpk and Fas mRNA expression

As our and other groups reported previously, inhibition of ChREBP transactivity was found to be beneficial for treating metabolic disorders in ob/ob mice [3,4]. A series of pcDNA6.2-Mlx mutants was constructed as shown in Fig. 1A and screened for dnMlx by analyzing Lpk promoter activity. Consistent with Fig. 1A, Mlx4-1 inhibited glucose-induced Lpk promoter activity by 60% (Fig. 1B). In contrast, Mlx2-1 increased Lpk promoter activity by 60% (Fig. 1B). As with the localization of Mlx mutants, Mlx2-1 was mainly localized in the nucleus, while Mlx4-1 and Mlx1-1 were localized in both the cytosol and nucleus (see Supplementary Fig. S1).

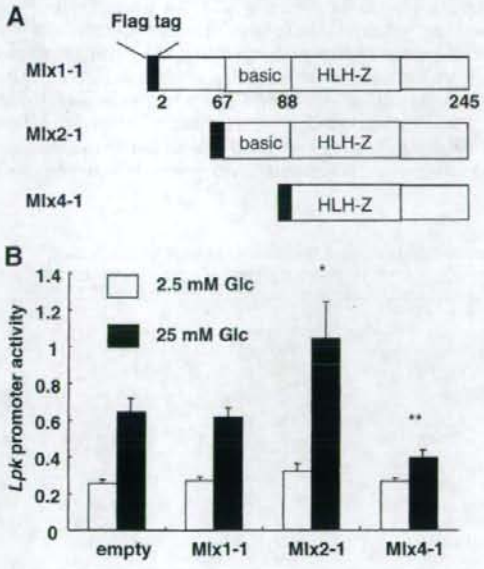

Fig. 1. (A) Schematic representation of wild-type Mlx (Mlx1-1), dominant active Mlx (Mlx2-1), and dominant negative Mlx (Mlx4-1). (B) Effects of Mlx1-1, Mlx2-1, or Mlx4-1 on Lpk promoter activity. Isolated hepatocytes were transfected with 3.6 μg of pGL3-Lpk, 0.4 μg of pGL4-TK-RLuc, and 0.4 μg of pcDNA6.2 empty, Mlx1-1, Mlx2-1, or Mlx4-1 vector using Lipofectamine 2000. Transfected cells were cultured for 24 h and used for analysis of luciferase activity. Data are means ± S.D. ($n = 6$ per group). *, $p < 0.05$ vs. pcDNA6.2 empty.

Mechanism by which Mlx4-1 inhibits ChREBP-mediated Lpk and Fasn gene expression

In the present study, a deletion mutant, Mlx4-1, was established that inhibits glucose-induced *Lpk* and *Fasn* gene expression. The effects of this mutant on *Lpk* and *Fasn* mRNA gene expression were evaluated. Consistent with Fig. 1B, Mlx4-1 dose-dendently inhibited glucose-induced *Lpk* and *Fasn* mRNA expression (Fig. 2A). When the Mlx4-1 mRNA level was increased 1680-fold, induction of these genes by glucose was completely blocked. The pGL3-3X*Lpk* and 3X*Fasn*-ChoRE vector were then used to clarify whether these inhibitory effects are due to binding of ChREBP/Mlx4-1 to ChoRE. Mlx4-1 completely inhibited ChREBP-regulated *Lpk* and *Fasn* reporter activity in rat hepatocytes (see Supplementary Fig. S2A). The inhibitory effects of Mlx4-1 on glucose-induced expression of *Chrebp* and *Transketolase* (*Tkt*) in rat primary hepatocytes were then examined. *Tkt* is an enzyme that forms xylulose-5-phosphate (Xu-5-P) from two glycolytic intermediates, glyceraldehyde 3-P (GAP) and fructose-6-P (Fru 6-P) (GAP + Fru 6-P ↔ Xu 5-P + erythrose 4-P) in the pentose phosphate pathway [1]. Xu-5-P activates

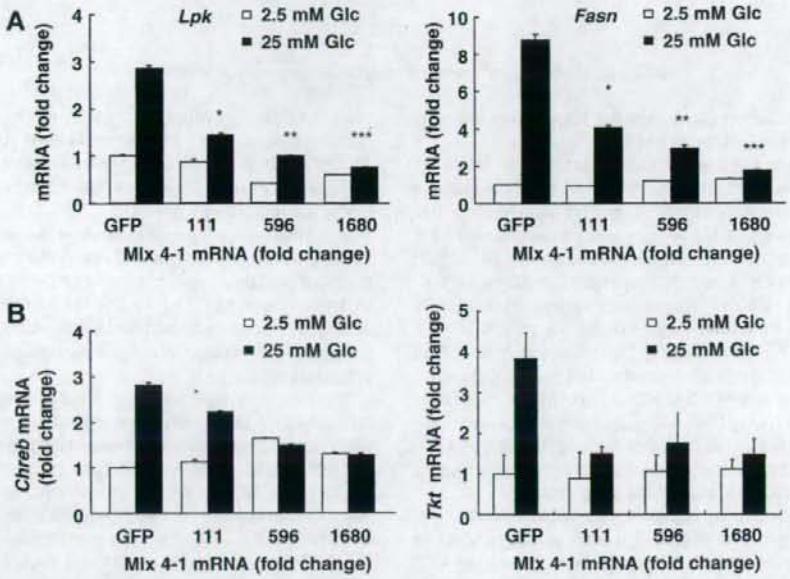

Fig. 2. (A) Overexpression of Mlx4-1 in rat hepatocytes inhibited glucose-induced *Lpk* and *Fasn* mRNA expression in a dose-dependent manner. *, **, *** $p < 0.05$ *vs.* GFP. (B) Mlx4-1 inhibited glucose-mediated *Chrebp* and *Tkt* mRNA induction in rat hepatocytes.

protein phosphatase 2A (PP2A), which in turn activates ChREBP by dephosphorylation [1]. Glucose stimulation was found to increase *Chrebp* and *Tkt* mRNA expression (see Supplementary Fig. S2B). Consistent with these data, a 1680-fold increase in Mlx4-1 completely inhibited glucose-induced *Chrebp* and *Tkt* mRNA expression in rat hepatocytes (Fig. 2B). These findings suggest that ChREBP and Tkt constitute a positive feedback loop involved in the regulation of glucose-mediated gene expression such as *Lpk* and *Fasn*.

Overexpression of Mlx4-1 improves glucose and lipid metabolism in diabetes-prone C57BL/6J mice

C57BL/6J mice develop metabolic syndrome with obesity and diabetes in response to a diet high in carbohydrate and/or fat [6]. Moreover, C57BL/6J mice develop glucose intolerance with age [6]. In this study, 25-week-old male C57BL/6J mice were used as a model diabetes-prone mouse to determine whether overexpression of Mlx4-1 improves glucose intolerance and other metabolic parameters in middle-aged C57BL/6J mice. Mice infected with Ad-GFP were used as controls. To minimize the side effects of adenovirus infection in the liver, all experiments were terminated after 5 days. Ad-Mlx4-1-injected mice appeared normal without hepatomegaly (Table 1). As shown in Table 1, body and tissue weights in Ad-Mlx4-1-infected mice were similar to those in controls. Ad-Mlx 4-1 overexpression did not affect food intake, as shown by stomach weight and food intake (Table 1). As shown in Table 2, AST and ALT concentrations were only slightly changed as compared with previously reported observations [4]. The delivery of 3×10^{13} particles/kg BW of Ad-Mlx4-1 or Ad-GFP adenovirus into C57BL/6J mice was liver-specific (data not shown). Increases of about 170-fold in endogenous Mlx mRNA levels were observed in livers infected with Ad-Mlx4-1 as compared with Ad-GFP (Fig. 3A). In liver overexpressing Ad-Mlx4-1, expression levels of the ChREBP target genes *Lpk* and *Fasn* were decreased by 84% and 65%, respectively, (Fig. 3A), suggesting that Mlx4-1 also functions as a dominant negative form of Mlx *in vivo*.

Liver triglyceride contents in Ad-Mlx4-1-injected mice were decreased by 40% due to decreased hepatic lipogenesis, but liver cholesterol contents were unchanged (Fig. 3B). Plasma lipid profile of Ad-Mlx4-1 mice was similar to that of controls (Table 2). Liver glycogen contents of Ad-Mlx4-1 mice were similar to controls (Fig. 3B). Plasma glucose concentration in Ad-Mlx4-1-injected mice was significantly decreased in both fasted and fed states (Table 2). In contrast, plasma insulin, triglyceride, and total cholesterol

Table 1
Phenotypic characteristics of 5-day-treated Ad-Mlx4-1 C57BL/6J mice.

	Ad-GFP	Ad-Mlx4-1
BW (g)	30.6 ± 2.1	30.4 ± 1.9
Food intake (g)	3.68 ± 0.26	3.60 ± 0.28
Stomach (%)	2.24 ± 0.26	2.04 ± 0.54
Liver (%)	5.8 ± 0.24	6.6 ± 0.73
White adipose tissue (%)	2.4 ± 1.4	1.6 ± 0.6
Kidney (%)	1.36 ± 0.14	1.45 ± 0.03

Data are means ± S.D. ($n = 5$ per group).

Table 2
Metabolic characteristics of 5-day-treated Ad-Mlx4-1 C57BL/6J mice.

	Ad-GFP	Ad-Mlx4-1	*P*-value
5-h fast			
Plasma glucose (mg/dl)	115 ± 6.2	81.4 ± 10.8*	$P = 0.014$
Plasma TG (mg/dl)	97.8 ± 22.1	89.6 ± 16.3	
Plasma T.Chol (mg/dl)	78.7 ± 10.1	81.5 ± 14.0	
18-h fast			
Plasma glucose (mg/dl)	86.2 ± 11	67.8 ± 6.6*	$P = 0.010$
Plasma insulin (ng/ml)	0.63 ± 0.21	0.43 ± 0.07	
Ad. lib. Fed			
Plasma glucose (mg/dl)	178 ± 34	111 ± 7.9*	$P = 0.019$
Plasma insulin (ng/ml)	0.83 ± 0.26	0.80 ± 0.26	
ALT (Units/l)	47.5 ± 16.6	93.9 ± 20.0*	$P = 0.010$
AST (Units/l)	32.3 ± 7.9	87.2 ± 14.2*	$P = 0.005$

Data are means ± S.D. ($n = 5$ per group). *$p < 0.05$ vs GFP. Abbreviations: ALT, alanine aminotransferase; AST, aspartate aminotransferase.

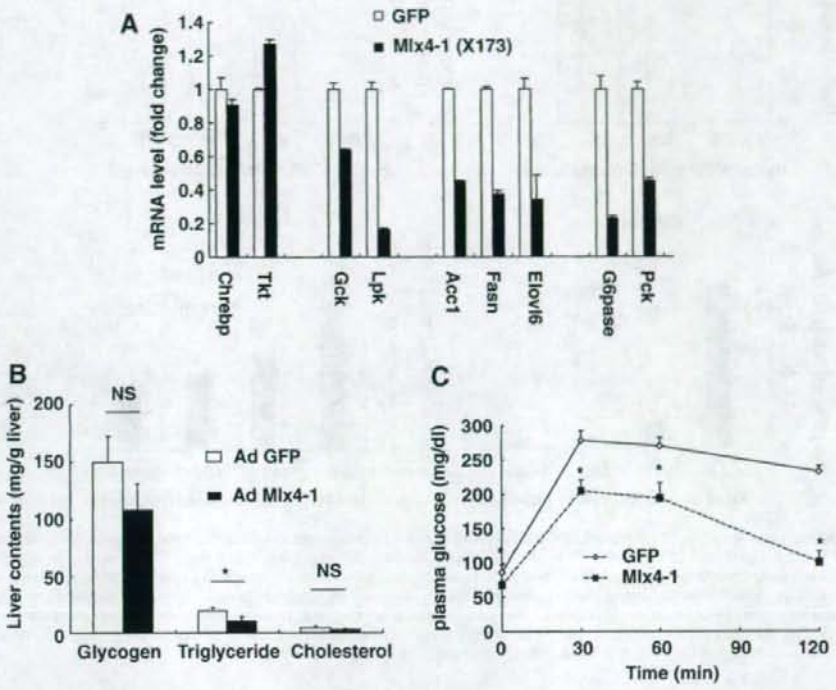

Fig. 3. (A) RT-PCR analysis of glycolytic, lipogenic, gluconeogenic, and lipolytic enzyme mRNA levels in liver of C57BL/6J mice infected with Ad-GFP or Ad-Mlx4-1. Results are means±SD ($n = 5$ per group). $p < 0.05$ vs. Ad-GFP injected C57BL/6J mice. (B) Determination of liver glycogen, triglyceride, and cholesterol contents in Ad-GFP or Ad-Mlx4-1 injected mice. Results are means±SD ($n = 5$ per group) $p < 0.05$ *vs.* Ad-GFP-injected mice. (C) Glucose tolerance tests (1 g/kg BW) were performed in C57BL/6J mice treated for 3 days with Ad-GFP or Ad-Mlx4-1 adenovirus. Animals were fasted for 18 h before OGTT ($n = 5$ per group). Data are means ± SD ($n = 5$ per group). $p < 0.05$ *vs.* Ad-GFP-injected C57BL/6J mice.

concentrations were similar to controls (Table 2). Consistent with these observations, oral glucose tolerance test showed that overexpression of Mlx4-1 improved glucose clearance from the body (Fig. 3C). In addition, glycolytic, lipogenic, and gluconeogenic gene mRNA expression levels were measured. As described above, glycolytic genes such as *Lpk* and lipogenic genes such as *Fasn*, *Acc1*, and ELOVL family member 6 (*Elovl6*) were suppressed by overexpression of Ad-Mlx4-1. In the gluconeogenesis pathway, glucose-6-phosphatase (*G-6-Pase*) and phosphoenolpyruvate carboxykinase (*Pepck*) mRNA levels were decreased by 80% and 50%, respectively, (Fig. 3C).

ChREBP induces G-6-Pase gene expression in rat hepatocytes

G-6-Pase gene expression is regulated by glucose signaling [7]. Moreover, Elovl6 is involved in lipid metabolism, and deletion of *Elovl6* improves glucose intolerance in ob/ob mice [8]. As shown in Fig. 3A, *G-6-pase* and *Elovl6* mRNA were down-regulated in the liver of Ad-Mlx4-1-injected mice. We therefore examined whether glucose and ChREBP can induce *G-6-Pase* and *Elovl6* mRNA in rat hepatocytes. Glucose increased hepatic *G-6-Pase* and *Elovl6* mRNA expression in a dose dependent manner (see Supplementary Fig. S4). Moreover, overexpression of dominant active ChREBP increased *G-6-Pase* and *Elovl6* mRNA expression in rat primary hepatocytes (Fig. 4A). Consistent with the findings shown in Fig. 4A, overexpression of dominant negative Mlx4-1 suppressed glucose-induced *G-6-Pase* and *Elovl6* mRNA expression (Fig. 4B). Thus, ChREBP regulates *G-6-Pase* and *Elovl6* gene expression in rat hepatocytes.

Discussion

This study was performed to determine whether hepatic inhibition of ChREBP transactivity can improve glucose intolerance in C57BL/6J mice. Overexpression of dnMlx/Mlx4-1 inhibited glucose-induced *Lpk*, *Fasn*, *Chrebp*, and *Tkt* gene expression in rat hepatocytes. Moreover, adenoviral delivery of dnMlx/Mlx4-1 into the liver improved glucose intolerance. Thus, blocking the association between ChREBP and Mlx is a promising therapeutic strategy to cure metabolic syndrome.

Mlx and ChREBP form the ChREBP-Mlx complex that binds ChoRE in glycolytic and lipogenic gene promoters such as *Lpk* and *Fasn*. Mlx4-1 is a dominant negative form of Mlx without the N-terminal and DNA-binding domains (Fig. 1A). Mlx4-1 is localized in both the cytosol and nucleus (see Supplementary Fig. S1). In contrast, Mlx2-1 is a dominant active form lacking only the N-terminal domain and is localized mainly in the nucleus. Consistent with our data, some groups have reported that the N-terminal domain of ChREBP has an important role in functions of ChREBP such as nuclear translocation and glucose sensitivity [9]. These observations suggest that the N-terminal domain of Mlx plays a role in determining glucose sensitivity and localization.

dnMlx/Mlx4-1 inhibits glucose-mediated *Lpk* and *Fasn* mRNA expression in rat hepatocytes. Towle et al. reported that Mlx plays an important role in glucose regulation of lipogenic enzymes, using their original Mlx mutant lacking only the DNA-binding domain, and obtained results compatible with ours [10]. Unlike their mutant, we constructed a mutant lacking both the N-terminal and the DNA-binding domains. Our observations suggest that the

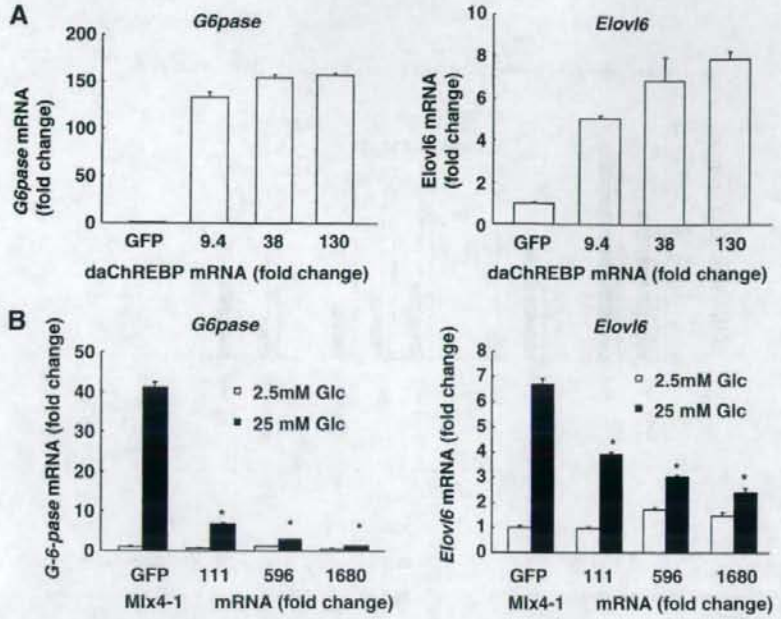

Fig. 4. (A) Adenoviral overexpression of dominant active ChREBP (daChREBP) induced *G-6-Pase* and *Elovl6* mRNA expression in rat hepatocytes. Adenovirus expressing either GFP or daChREBP was transduced into rat hepatocytes at m.o.i. of 2, 10, or 50. As control, a recombinant adenovirus expressing GFP was used at m.o.i. of 50. Two h after infection, cells were kept in DMEM including 2.5 mM glucose for an additional 18 h. Total RNA was then extracted from hepatocytes and RT-PCR analysis was performed. Values represent means±S.D. $^{*}p < 0.05$ *vs.* Ad-GFP. (B) Adenoviral overexpression of Mlx4-1 inhibited glucose-stimulated *G-6-Pase* and *Elovl6* mRNA expression in rat hepatocytes. Adenovirus overexpressing either GFP or Mlx4-1 was transduced into rat hepatocytes at m.o.i. of 2, 10, or 50. As control, a recombinant adenovirus expressing GFP was used at m.o.i. of 50. Two h after infection, cells were kept in DMEM including glucose concentrations of 2.5 or 25 mM for an additional 18 h. Total RNA was then extracted from hepatocytes and RT-PCR analysis was performed. Values represent means±S.D. $^{*}p < 0.05$ *vs.* Ad-GFP.

DNA-binding domain is critical in transactivity of Mlx. Moreover, dnMlx/Mlx4-1 inhibited activation of *Chrebp* and *Tkt* mRNA expression by glucose. In the pentose pathway, glucose is converted to Xu-5-P, an activator of ChREBP [1]. As Xu-5-P is produced by Tkt, ChREBP and Tkt constitutes a positive feedback loop by increasing *Tkt* and *ChREBP* mRNA in rat hepatocytes. It is surprising that glucose increases *Chrebp* mRNA expression in rat hepatocytes and the mechanism remains unknown. Using dnMlx-expressing adenovirus vector, ChREBP was found to directly regulate *Chrebp* gene expression. However, *Tkt* and *Chrebp* mRNA levels were not decreased in the livers of Ad-Mlx4-1-injected mice. In contrast, overexpression of daChREBP caused 40- and 14-fold increases in endogenous *Chrebp* and *Tkt* mRNA levels, respectively, (data not shown). Thus, while glucose regulates *Tkt* and *ChREBP* mRNA expression in rat hepatocytes, other factors may regulate their gene expression more potently *in vivo*.

We and other groups have independently reported that gene deletion or shRNA of *Chrebp* improves metabolic disorders in ob/ob mice [3,4]. However, complete deletion of *Chrebp* causes massive hepatomegaly due to liver glycogen accumulation [3]. Moderate inhibition of ChREBP transactivity thus might improve the symptoms of metabolic syndrome without hepatomegaly. In rat hepatocytes, Mlx4-1 functions only at higher glucose concentrations. In contrast, *Chrebp* gene deletion or *Chrebp* shRNA works at both lower and higher glucose concentrations. Since this is a unique characteristic of dnMlx/Mlx4-1, we tested 25-week-old diabetes-prone C57BL/6J mice. The C57BL/6J mouse is a model of diet-induced obesity and diabetes [6]. As C57BL/6J mice develop glucose intolerance with age similarly to humans, middle-aged C57BL/6J mice were used to test the effects of dnMlx on improvement of glucose intolerance. Overexpression of dnMlx/Mlx4-1 improved glucose intolerance and liver lipid contents without hepatomegaly. These observations suggest that drugs disrupting the association between ChREBP and Mlx may be promising for preventing the development of metabolic syndrome.

dnMlx/Mlx4-1 inhibited expression of genes encoding the glycolytic enzyme *Lpk*, lipogenic enzymes *Acc1*, *Fasn*, and *Elovl6*, and gluconeogenic enzyme *G-6-Pase*, although the precise mechanism by which inhibition of ChREBP transactivity improves metabolic syndrome remains unknown. Elovl6 catalyzes conversion of palmitate to stearate [8]. Consistent with Fig. 4B, dnMlx inhibited glucose-induced *Elovl6* gene expression in primary hepatocytes [11]. Gene deletion of *Elovl6* in high-fat-loaded mice or ob/ob mice improved glucose intolerance by modifying hepatic fatty acid composition, but did not improve hepatic steatosis [8]. We did not analyze hepatic fat composition in Ad-Mlx4-1-injected mice, but fat composition in Chrebp$^{-/-}$ mice was similar to that in normal controls (unpublished data). Moreover, glucose clearance in *Elovl6* knockout mice was similar to that in controls [8]. Thus, *Elovl6* mRNA may contribute to improvement of glucose intolerance, even though its effect in Ad-dnMlx/Mlx4-1 mice is limited.

DnMlx inhibited glucose induction of *G-6-pase* mRNA expression. Acute inhibition of the G-6-Pase system lowers the plasma glucose concentration in rats [12]. These observations suggest that G-6-Pase plays an important role in glucose homeostasis in rodents. Some groups have reported the possibility that ChREBP binds to ChoRE in the rat *G-6-Pase* promoter region [7]. Fig. 4A and B indicates that glucose and ChREBP strongly regulate *G-6-pase* gene expression in rat hepatocytes. As SREBP1c did not regulate *G-6-Pase* mRNA expression, and deletion of SREBP1c did not improve glucose intolerance, the difference in *G-6-pase* gene regulation be-

tween ChREBP and SREBP may underlie the improvement of glucose intolerance by ChREBP but not by SREBP [1].

In conclusion, experiments using dnMlx/Mlx4-1 indicate that ChREBP is regulated by *Chrebp* and *Tkt* gene expression, and forms a positive feedback loop in rat hepatocytes. Moreover, overexpression of dominant negative Mlx improves glucose intolerance in diabetes-prone C57BL/6J mice with metabolic syndrome. These observations suggest that drugs capable of dissociating the ChREBP-Mlx complex may be a promising approach to treatment of metabolic syndrome including glucose intolerance.

Acknowledgments

This work was supported by Grants-in-Aid for Scientific Research from the Japan Society for the Promotion of Science (K. Iizuka), the ONO Medical Research Foundation (K. Iizuka), the Kao Research Council for the Study of Healthcare Science (K. Iizuka), and in part by a New Energy and Industrial Technology Development Organization grant (Y. Horikawa). We apologize to authors whose work was not been cited because of limited space.

Appendix A. Supplementary data

Supplementary data associated with this article can be found, in the online version, at doi:10.1016/j.bbrc.2008.12.100.

References

[1] K. Iizuka, Y. Horikawa, ChREBP: a glucose-activated transcription factor involved in the development of metabolic syndrome, Endocr. J. 55 (2008) 617–624.

[2] H. Shimano, Sterol regulatory element binding proteins (SREBPs): transcriptional regulators of lipid synthetic genes, Prog. Lipid. Res. 40 (2001) 439–452.

[3] K. Iizuka, B. Miller, K. Uyeda, Deficiency of carbohydrate-activated transcription factor ChREBP prevents obesity and improves plasma glucose control in leptin-deficient (ob/ob) mice, Am. J. Physiol. Endocrinol. Metab. 291 (2006) E358–364.

[4] R. Dentin, F. Benhamed, I. Hainault, V. Fauveau, F. Foufelle, J.R. Dyck, J. Girard, C. Postic, Liver-specific inhibition of ChREBP improves hepatic steatosis and insulin resistance in ob/ob mice, Diabetes 55 (2006) 2159–2170.

[5] K. Iizuka, Y. Horikawa, Regulation of lipogenesis via BHLHB2/DEC1 and ChREBP feedback looping, Biochem. Biophys. Res. Commun. 374 (2008) 95–100.

[6] A.E. Petro, J. Cotter, D.A. Cooper, J.C. Peters, S.J. Surwit, R.S. Surwit, Fat, carbohydrate, and calories in the development of diabetes and obesity in the C57BL/6J mouse, Metabolism 53 (2004) 454–457.

[7] K.B. Pedersen, P. Zhang, C. Doumen, M. Charbonnet, D. Lu, C.B. Newgard, J.W. Haycock, A.J. Lange, D.K. Scott, The promoter for the gene encoding the catalytic subunit of rat glucose-6-phosphatase contains two distinct glucose-responsive regions, Am. J. Physiol. Endocrinol. Metab. 292 (2007) E788–801.

[8] T. Matsuzaka, H. Shimano, N. Yahagi, T. Kato, A. Atsumi, T. Yamamoto, N. Inoue, M. Ishikawa, S. Okada, N. Ishigaki, H. Iwasaki, Y. Iwasaki, T. Karasawa, S. Kumadaki, T. Matsui, M. Sekiya, K. Ohashi, A.H. Hasty, Y. Nakagawa, A. Takahashi, H. Suzuki, S. Yatoh, H. Sone, H. Toyoshima, J. Osuga, N. Yamada, Crucial role of a long-chain fatty acid elongase, Elovl6, in obesity-induced insulin resistance, Nat. Med. 13 (2007) 1193–1202.

[9] M.V. Li, B. Chang, M. Imamura, N. Poungvarin, L. Chan, Glucose-dependent transcriptional regulation by an evolutionaly conserved glucose-sensing module, Diabetes 55 (2006) 1179–1189.

[10] L. Ma, L.N. Robinson, H.C. Towle, ChREBP·Mlx is the principal mediator of glucose-induced gene expression in the liver, J. Biol. Chem. 281 (2006) 28721–28730.

[11] Y. Wang, D. Botolin, J. Xu, B. Christian, E. Mitchell, B. Jayaprakasam, M.G. Nair, J.M. Peters, J.V. Busik, L.K. Olson, D.B. Jump, Regulation of hepatic fatty acid elongase and desaturase expression in diabetes and obesity, J. Lipid. Res. 47 (2006) 2028–2204.

[12] J.C. Parker, M.A. VanVolkenburg, C.B. Levy, W.H. Martin, S.H. Burk, Y. Kwon, C. Giragossian, T.G. Gant, P.A. Carpino, R.K. McPherson, P. Vestergaard, J.L. Treadway, Plasma glucose levels are reduced in rats and mice treated with an inhibitor of glucose-6-phosphate translocase, Diabetes 47 (1998) 1630–1636.

doi: 10.1507/endocrj.K08E-302

Advance Publication

ORIGINAL

Identification of Minimal Promoter and Genetic Variants of Kruppel-like Factor 11 Gene and Association Analysis with Type 2 Diabetes in Japanese

Eiji KURODA[1], Yukio HORIKAWA[1,2], Mayumi ENYA[1], Naohisa ODA[3], Eiji SUZUKI[1], Katsumi IIZUKA[2] and Jun TAKEDA[1]

[1]Department of Diabetes and Endocrinology Division of Molecule and Structure, Gifu University School of Medicine, Gifu, [2]Laboratory of Medical Genomics, Biosignal Genome Resource Center, Institute for Molecular and Cellular Regulation, Gunma University, Maebashi, [3]Department of Internal Medicine, Fujita Health University School of Medicine, Aichi, Japan

Received October 21, 2008; Accepted December 12, 2008; Released online December 27, 2008

Correspondence to: Yukio HORIKAWA, MD, PhD, Department of Diabetes and Endocrinology, Division of Molecule and Structure, Gifu University School of Medicine, Gifu

Abstract. Genetic analysis of the KLF11 gene revealed two rare variants, A347S and T220M, segregating in families with early-onset type 2 diabetes, and one frequent polymorphic Q62R variant significantly associated with type 2 diabetes in Northern Europeans. Furthermore, it has been reported that over-expression of *KLF11* has a deleterious effect on insulin promoter activity. Thus, an altered expression level of *KLF11* may contribute to the occurrence of type 2 diabetes. To investigate the contribution of KLF11 to type 2 diabetes in Japanese, we surveyed the 5' flanking region of *KLF11* by reporter assay and identified the minimal promoter region of the gene. The promoter region from -250 to +162bp including five Sp1 binding sites showed basal promoter activity both in MIN6-m9 and HepG2 cells. We also examined the entire region of *KLF11* to detect genetic variants. A total of 19 polymorphisms, six of which are novel, were identified, but none of them showed association with the occurrence of type 2 diabetes. Two of the identified polymorphisms, R29Q and S124F, are novel coding variants. Functional analyses of these variants were performed, and similarly reduced effects on transcriptional activities of insulin, catalase1, and the Smad7 gene were found. We conclude that variants of *KLF11* are not a major factor in the occurrence of type 2 diabetes in Japanese. The promoter region of *KLF11* identified in the present study should be useful in further elucidation of the transcriptional regulation mechanism of the gene and genetic analyses of type 2 diabetes.

Key words: KLF11, SNP, association study, promoter, type 2 diabetes

KRUPPEL-LIKE transcription factor (KLF)11 (also known as TIEG2) is a member of the Sp1-like transcription factor family, which is defined by the presence of three conserved DNA-binding C-terminal zinc finger domains and variant N-terminal domains [1–4]. In contrast with Sp1, one of the best–characterized transcriptional activators, KLF11 behaves as a potent transcriptional repressor. KLF/Sp1-like transcription regulation may participate in many aspects of cellular function, including cell proliferation, apoptosis, differentiation, and neoplastic transformation [5–8].

The KLF11 gene is located at chromosome 2p25 [9], and is ubiquitously expressed in human tissues with an abundance in pancreas and muscle [4]. KLF11 has elicited significant attention due to its role as a negative regulator of exocrine cell growth by decreasing growth and increasing apoptosis via a mechanism that involves down-regulation of the oxidative stress genes SOD2 and catalase1 [10], which also are expressed in pancreatic islets, and an increased susceptibility to oxidative insult [11]. The

Smad-regulated transcriptional pathway plays a central role in TGF-β induced cell growth inhibition [12]. Smad signaling activity is potentiated by KLF11 in normal epithelial cell lines through termination of the negative feedback loop imposed by Smad7, which requires binding to GC-rich promoter boxes of the Smad7 promoter [13], and the TGF-β signaling pathway is a major regulator of endocrine cell fate [14–16].

The role of KLF11 within the endocrine pancreas remains to be elucidated. Recently, Neve et al. reported that KLF11 binds to the insulin promoter and up-regulates its activity in beta-TC3 cells. Genetic analysis of *KLF11* revealed two rare variants (Ala347Ser and Thr220Met) that segregate with diabetes in families with early-onset type 2 diabetes (T2DM) and significantly impair its transcriptional activity [17]. On the other hand, Niu et al reported that over-expression of hKLF11 inhibits the activity of human insulin promoter in INS-1E and beta-TC3 cells in a dose-dependent and glucose-independent manner [18]. Furthermore, it has been reported that a *KLF11* promoter variant has a deleterious effect on insulin sensitivity via STAT3-mediated up-regulation of *KLF11* [19]. Thus, an altered expression level of *KLF11* may contribute to the occurrence of type 2 diabetes.

In this study, we surveyed the 5' flanking region of *KLF11* and identified the minimal promoter region of the gene, which should be useful in further genetic and functional analyses of type 2 diabetes. We also examined all of the regions of *KLF11* in twelve Japanese subjects to detect genetic variants, evaluated the pattern of linkage disequilibrium to infer haplotypes in the gene, and performed association studies with type 2 diabetes patients.

Material and methods

Subjects

A total of 182 Japanese subjects with clinical diagnosis of early-onset type 2 diabetes (70 males and 112 females; onset age 11.9 ± 3.1yr, BMI, 23.9 ± 6.2kg/m^2; onset HbA1c 8.8 ± 3.1 %, HbA1c 7.1 ± 2.3 %)) were screened for mutations by direct sequencing of PCR products. Patients with glutamic acid decarboxylase (GAD) antibodies and other types of diabetes were excluded on the basis of clinical data.

A total of 553 Japanese patients with late-onset T2DM [310 males and 243 females; age at testing, 61.1 ± 10.6 yr; BMI, 23.9 ± 4.1 kg/m2; glycosylated hemoglobin (HbA1c), 7.7 ± 3.5%] and 563 controls (224 males and 339 females; age at testing 67.4 ± 6.0yr; BMI, 22.9 ± 2.9 kg/m^2; HbA1c, 5.0 ± 0.4%) were examined for association study. The diagnosis of T2DM was based on medical records or 75g oral glucose tolerance test according to the criteria of the Japan diabetes Society [20]. Informed consent was obtained from all of the diabetic subjects and volunteer controls. The study was approved by the ethics committee of Gifu University.

SNP identification in KLF11

Genomic DNA was extracted from samples of whole blood using QIAamp DNA blood kit (QIAGEN, Hilden, Germany) according to the manufacturer's instructions. Twelve of the random control samples (24 alleles) were used to detect SNPs in *KLF11*. Primers for PCR experiments were designed by Primer3 (available from http://www.genome.wi.mit.edu/cgi-bin/primer/preimer3 www.cgi) on the basis of the genomic contig sequence (GenBank ID: NT_005334.15, nt 5016199 - 5029771bp) of the *KLF11* region. The mixture for PCR was 20μl in 10ng template DNA, 0.5 mM of each dNTP, 2.5 pmol of each forward and reverse primer, 0.5 U ExTaq polymerase (Takara,Kyoto,Japan), and 2μl of 10 x PCR buffer or 0.4 U KOD FX (TOYOBO,OSAKA,JAPAN) and 10μl of 2xPCR buffer for KOD FX. The reaction conditions with Ex Taq polymerase were an initial denaturation step of 94°C for 1min and